



A proposed chronostratigraphic Archean–Proterozoic boundary: Insights from the Australian stratigraphic record

David McB Martin^{a,*}, Indrani Mukherjee^b, Alex J. McCoy-West^{c,d}, Heather M. Howard^a

^a Geological Survey of Western Australia, 100 Plain Street, East Perth, WA 6004, Australia

^b School of Biological, Earth and Environmental Sciences, University of New South Wales, Sydney NSW 2052, Australia

^c IsoTropics Geochemistry Laboratory, Earth and Environmental Science, James Cook University, Townsville, 4811, Australia

^d Economic Geology Research Centre, James Cook University, 1 James Cook Drive, Townsville, QLD 4811, Australia

ARTICLE INFO

Keywords:

Archean
Proterozoic
Precambrian
pre-Cryogenian
Chronometric
Chronostratigraphic
GOE

ABSTRACT

The Mount Bruce Supergroup (MBS) in Western Australia has been central to debates surrounding Precambrian stratigraphic subdivision and is one of the few relatively conformable successions that records both the chronometric Archean-Proterozoic boundary (APB) and the Great Oxidation Event/Episode (GOE) which has previously been proposed as the most practical basis for a chronostratigraphic boundary. Current understanding of the lithostratigraphy, chemostratigraphy, and geochronology of the MBS supports the placement of a chronostratigraphic APB in the vicinity of the contact between the Hamersley and Turee Creek Groups, although a precise boundary awaits the generation and integration of more detailed chemostratigraphic records of the GOE with the physical record. The chronometric APB as presently defined at 2500 Ma will suffice until consensus is reached regarding a revised definition based on the GOE, and reconciliation of the physical and proxy records of this event. However, the Australian stratigraphic record suggests placement of the APB either at the base of the first glacial diamictite, or at the top of the last banded iron formation (BIF) below the GOE. The first option would exclude some BIF from the Siderian, which in both cases would be the terminal period of the Archean, whereas the second option places all diamictite in a new period at the start of the Paleoproterozoic. It is further proposed that this new period be named to primarily reflect this glacial influence, rather than for the influence of the GOE which relies on less obvious laboratory-based proxies for its identification.

1. Introduction

The Archean–Proterozoic boundary (APB) has long been interpreted to reflect a fundamental change in Earth surface processes and environments, although its precise definition and assigned age have changed as understanding of the geological evolution of Earth has matured. Much of this improvement in understanding has been driven over the last three decades by an explosion in precise U–Pb zircon ages, supported more recently by a similar expansion of novel geochemical and isotopic data. One consequence of the improved geochronological constraints on the physical stratigraphic record has been to highlight the limitations and impracticalities of current Global Standard Stratigraphic Ages (GSSAs) for the Precambrian. This has led to increasing calls either for alternative stratigraphic approaches, or revisions that would more closely align individual GSSAs with the physical rock record (Bleeker, 2004; Cloud, 1987; Condie and O'Neill, 2010; Robb et al., 2004; Shields et al., 2022;

Van Kranendonk et al., 2012). The latter approach is presently implemented via the definition of Global Stratotypes Sections and Points (GSSPs) for the post-Cryogenian (Cohen et al., 2013).

The chronometric APB at 2500 Ma has served the Precambrian geoscience community adequately for over thirty years; however, it has not been without its critics who have advocated for a chronostratigraphic boundary that is better aligned with the rock record. The International Commission for Stratigraphy has embraced this approach in defining the terminal periods of the Precambrian, the Cryogenian and Ediacaran, and is in the process of extending chronostratigraphic subdivision throughout the pre-Cryogenian. The pre-Cryogenian Sub-commission is currently focused on subdivision of the Archean, and definition of its boundary with the Hadean. Definition of a chronostratigraphic APB is a critical element of this effort that has not yet been formally debated or ratified, although this boundary is arguably of equal or greater geological significance to the base Phanerozoic and

* Corresponding author.

E-mail address: david.martin@dmirs.wa.gov.au (D. McB Martin).

<https://doi.org/10.1016/j.precamres.2024.107377>

Received 10 January 2024; Received in revised form 20 March 2024; Accepted 26 March 2024

Available online 6 April 2024

0301-9268/Crown Copyright © 2024 Published by Elsevier B.V. This is an open access article under the CC BY license (<http://creativecommons.org/licenses/by/4.0/>).

Archean.

The Australian stratigraphic record has always been important in informing the debates surrounding Precambrian stratigraphy (e.g. Dunn et al., 1966; Plumb and James, 1986; Trendall, 1984). Specifically, the Mount Bruce Supergroup (MBS) in Western Australia has special relevance to the definition of the APB since it is one of the few conformable successions globally to contain the 2500 Ma chronometric boundary (Fig. 1). For this reason and following the proposed revisions to the Precambrian timescale by Van Kranendonk et al. (2012), a dedicated session and associated fieldtrip to examine the Archean-Proterozoic transition were held at the 6th International Archean Symposium (6IAS) in Fremantle, Western Australia (25–27th July 2023). Unfortunately, this session did not attract the anticipated level of participation, no doubt exacerbated by delays due to the COVID-19 pandemic. However, this paper summarises some of the key observations from the conference that are relevant to the debate surrounding proposals for a revised APB, along with relevant recent advances in geological

understanding of the MBS that were presented on the associated post-conference fieldtrip (Martin and Howard, 2023) and may be significant to any considerations of a revised global definition of the APB. The implications of important new studies that have been published since the field excursion (Havsteen et al., 2023; Senger et al., 2023; Uveges et al., 2023) have also been considered in the global correlation

2. The rationale for change

Debate surrounding appropriate approaches to the subdivision of Precambrian time, including recognition of discrete Archean, Proterozoic and Hadean Eons, has a long pedigree most recently summarized by Shields et al. (2022). The current approach of the International Commission on Stratigraphy (ICS) for subdivision of Precambrian time that uses a combination of ratified and informal GSSAs to define chronometric intervals, that in turn delimit interpreted major episodes of sedimentation, orogeny and magmatism (Fig. 2), has been in use for

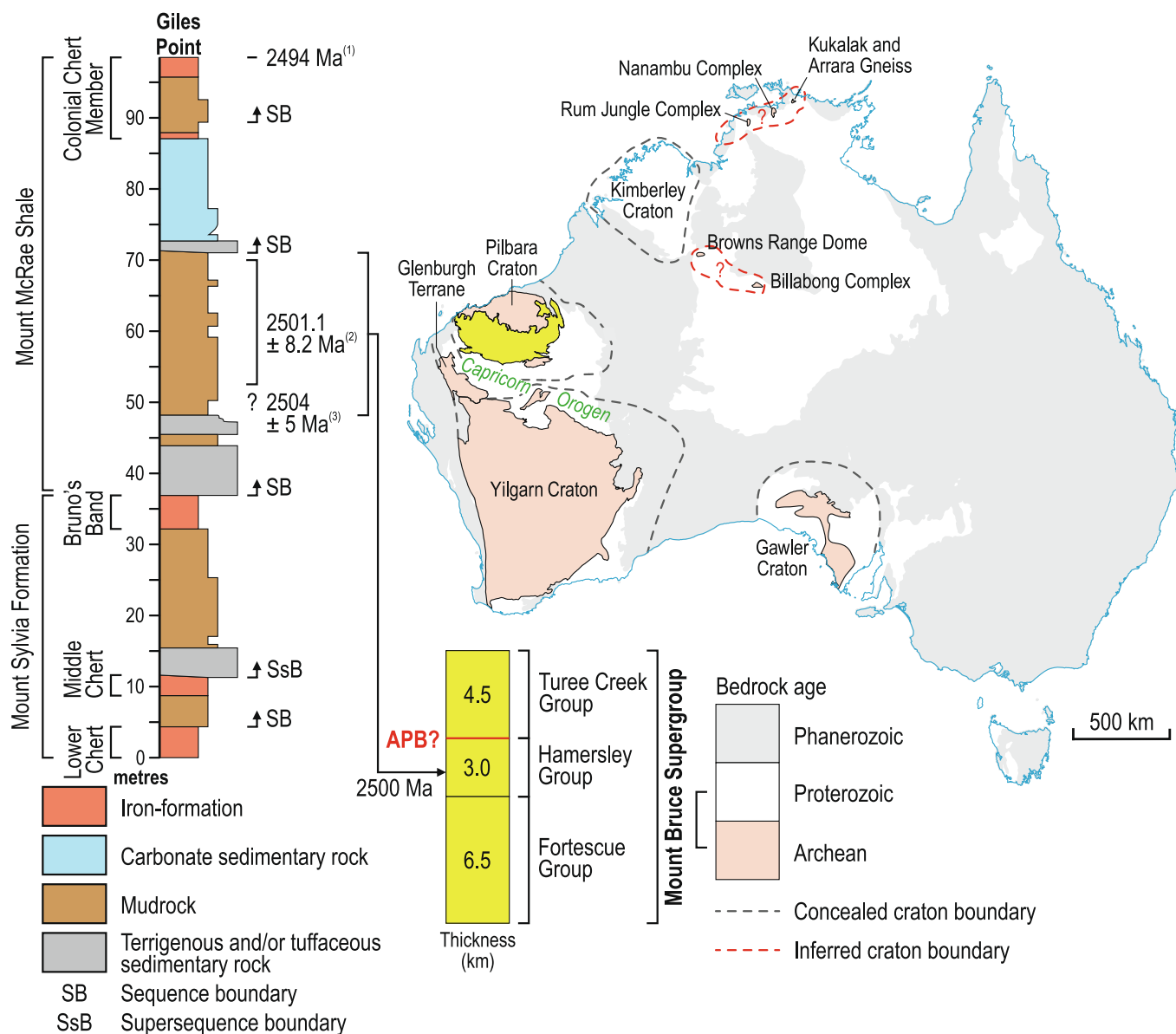


Fig. 1. Geological setting of the Mount Bruce Supergroup, that contains both the 2500 Ma chronometric and the chronostratigraphic Archean–Proterozoic boundary (APB?) proposed by Van Kranendonk et al. (2012) in the context of the Australian bedrock age map. The main named Archean cratonic nuclei are also shown (after Tyler, 2005; Cawood and Korsch, 2008), as well as two unnamed cratons inferred from limited outcrop. The lithostratigraphic and sequence stratigraphic location of the chronometric APB and its age constraints is shown by reference to a section at Giles Point (simplified after Krapez et al., 2003). Ages are from 1) Trendall et al. (2004), 2) Anbar et al., (2007), and 3) Rasmussen et al. (2005).

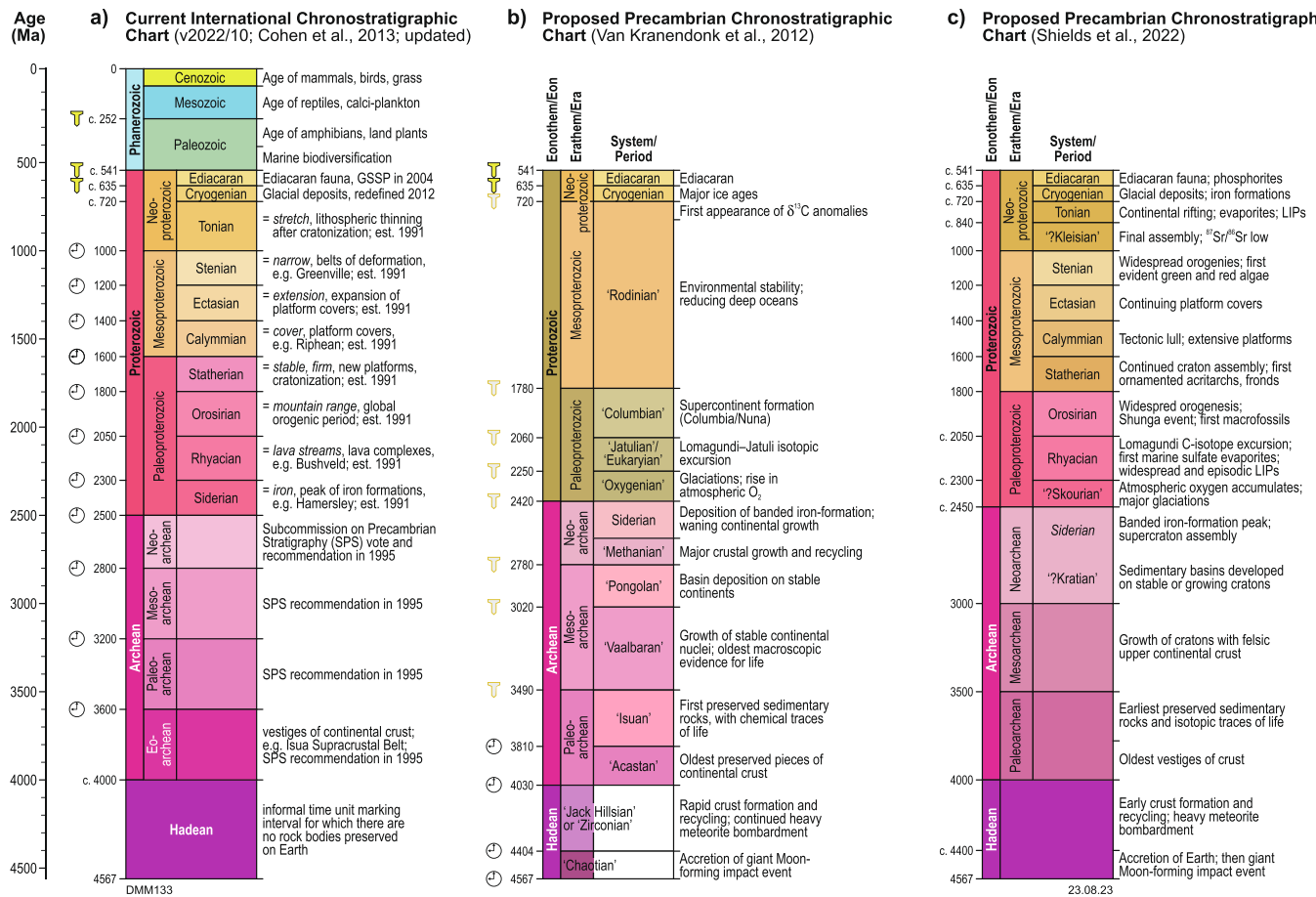


Fig. 2. Comparison of the current ICS geological timescale with recently proposed revisions for the Precambrian: a) current geological timescale (after Cohen et al., 2013; Strachan et al., 2020); b) proposed Precambrian revisions of Van Kranendonk et al. (2012); c) proposed Precambrian revisions of Shields et al. (2022). Yellow golden spike symbols represent ratified (bold) and potential (pale) GSSPs. Clock symbols represent ratified Proterozoic and recommended Archean GSSAs. Proposed era and period ages in b) and c) are approximate and are likely to change in any ratified chronostratigraphic scheme; proposed informal period names are listed in inverted commas. Figure modified after Shields et al. (2022). (For interpretation of the references to colour in this figure legend, the reader is referred to the web version of this article.)

many decades (Plumb, 1991; Plumb and James, 1986). However, revisions to this primarily chronometric approach to Precambrian subdivision have recently been suggested in an effort to more closely align temporal subdivisions with the available and preserved rock record (e.g. Shields et al., 2022; Van Kranendonk et al., 2012). Such a chronostratigraphic approach has been proposed in response to the significant recent advances in understanding early Earth history, and the more detailed and precise geological, geochronological, and geochemical constraints that are now available.

Objections to the recommended chronometric approach of the ICS (Plumb and James, 1986) were soon raised by Cloud (1987), but after initial ratification (Plumb, 1991) the GSSP approach used for the Phanerozoic rock record was subsequently extended into the Precambrian following ratification of the boundaries of the Ediacaran (Knoll et al., 2004) and Cryogenian (Shields-Zhou et al., 2016) Periods. Consequently, the pre-Cryogenian Sub-commission (formerly Sub-commission on Precambrian Stratigraphy) of the ICS is now considering extending chronostratigraphic sub-division throughout the pre-Cryogenian. Although this approach was explicitly rejected by Plumb and James (1986), current understanding of Earth history has precipitated a reconsideration.

The APB was originally chosen as an arbitrary whole number at 2500 Ma, although this choice was informed by known geological history at the time to avoid splitting major cratonization events (James, 1978). This definition was subsequently ratified (Plumb and James,

1986; Plumb, 1991), and later finer subdivision of the Precambrian also involved this mixed approach in which boundaries were assigned GSSAs that in turn delimit major episodes of sedimentation, orogeny, and magmatism. The age chosen for the APB was originally based on K–Ar ages, later revised with U–Pb and Rb–Sr ages (James, 1978) and reflected temporal constraints on regional metamorphism in the Northern Hemisphere at the time of proposal by Plumb and James (1986). The extensive Precambrian geochronological database that has been amassed since, that covers a wide range of geochronometers, warrants a re-evaluation of the age of this boundary along with its chronostratigraphic definition based on current geological understanding.

The current approach to Precambrian subdivision has many limitations and has been the subject of repeated criticism over the years (e.g. Bleeker, 2004; Cloud, 1987; Crook, 1989; Hofmann, 1990) that has led to the recent push towards more precise chronostratigraphic definitions via extension of GSSP definitions into the pre-Cryogenian. The two most common approaches to Precambrian chronostratigraphic subdivision relate to units based either on changes to the physical Earth (e.g. orogenic episodes or tectonic style) or to changes in surface conditions or processes (e.g. fundamental biospheric changes). These each have their merits, but the consensus for an APB definition seems to have swung away from the former (e.g. Blake and Groves, 1987; Condie and O’Neill, 2010; Plumb and James, 1986) and towards the latter (e.g. Shields et al., 2022; Van Kranendonk et al., 2012).

Regardless of the approach taken, the event chosen to demarcate the

APB should have a physical manifestation similar in magnitude or significance to the explosion and preservation of macroscopic life at the Cambrian–Precambrian boundary. Furthermore, the APB and the finer subdivisions of the pre-Cryogenian need to have practical mapping application such that analytical data are not the primary basis for unit/boundary identification and correlation. This includes absolute time constraints, such that radiometric ages should calibrate events and boundaries rather than define them, as originally proposed by Cloud (1987, 1976). As pointed out by Plumb and James (1986), the need for a Precambrian timescale relates more to effective communication than necessity, and to this end the subdivisions and their boundaries should carry clear geological meaning. This was the intent of the original definitions, but significant improvements in geological understanding and calibration of the rock record since then has diminished their effectiveness for communication.

2.1. Limitations of the current approach

The primary criticism of the ratified ICS approach to pre-Cryogenian stratigraphic subdivision is that it mixes chronometry (division according to time alone) and chronostratigraphy (division into time-rock units), via selection of boundaries based on cycles of sedimentation, orogeny and magmatism but defined in years without reference to any rock bodies (Plumb and James, 1986). A full account of the criticisms of this aspect of the Plumb and James (1986) approach is beyond the scope of this contribution, and has already been reviewed elsewhere (e.g. Cloud, 1987; Gradstein et al., 2004; Van Kranendonk et al., 2012; Shields et al., 2022). However, there are two practical limitations that have particular relevance to the Mount Bruce Supergroup (MBS). First is the fact that the chronometric APB (i.e. 2500 Ma) in the MBS is located within a relatively monotonous lithostratigraphic unit (Fig. 1), the practical implication of which is that in Australia the Archean and Proterozoic Eonothems cannot be accurately mapped without splitting the Mount McRae Shale. This may be considered a relatively minor limitation compared to the significance of the 2500 Ma boundary to current understanding of geological evolution across an interpreted Archean–Proterozoic transition or boundary. Secondly, the concept of a ‘transition’ in Earth history between the Archean and Proterozoic Periods is well established (Cloud, 1987; Gradstein et al. 2004; Condie and O’Neill, 2010) but is not readily apparent in the MBS (Trendall, 1984). Definitions of this transition have changed over time (e.g. Plumb and James, 1986; Cloud, 1987; Gradstein et al., 2004; Condie and O’Neill, 2010) and depend on the perspective from which it is viewed. The boundary was originally defined based on a solid earth perspective, whereas more recent proposals have tended to lean more towards a boundary defined by changes to surface conditions. The stratigraphic record of the MBS provides critical insight for both these perspectives.

2.2. Solid Earth changes

Since the accretion of Earth from the protoplanetary disc, the geosphere has experienced many long-term changes such as bulk cooling, extraction of the continental crust from the mantle, and stabilisation of major cratons that have in turn affected processes such as tectonic style (Bédard, 2018; Cawood et al., 2013; McCoy-West et al., 2019). Such changes to the solid Earth have formed the basis of many schemes of Precambrian stratigraphic subdivision, including that of Plumb and James (1986) who designated the Archean as a rock unit characterised by granite-greenstones and high-grade gneiss terranes, with 2500 Ma marking the beginning of a major tectono-magmatic lull that followed a period of extensive cratonization (James, 1978). However, cratonization has since been shown to be diachronous (Blake and Groves, 1987; Cawood et al., 2018; Cheney et al., 1990; Cloud, 1976; Young, 1978) and the consequences of the interpreted tectono-magmatic lull after 2500 Ma are not clear in the MBS (Trendall, 1984). On the contrary, from the Australian perspective, this period is characterised by active tectonism

and magmatism in an interpreted back-arc setting (Barley et al., 1997; Blake and Barley, 1992; Trendall, 1995).

2.3. Changing surface conditions

Most recent proposals for a change in the criteria used to define the APB focus on changes to the atmosphere, biosphere and hydrosphere that are more likely to be globally synchronous on geological timescales because of their faster homogenisation rates. A suite of geochemical proxies, using both conventional and in-situ techniques, have been developed over the years to track atmosphere–ocean redox conditions, particularly during the Archean–Proterozoic transition (Lyons et al., 2021). Unfortunately, these changes are difficult to pinpoint in the rock record because they rely on analytical proxy records that are inevitably incomplete and therefore difficult to correlate such as the sulfur isotope record discussed below. Furthermore, different proxies yield different results and by extension varied interpretations. For instance, some studies advocate for a sharp rise of atmospheric oxygen (O_2) at c. 2.33 Ga (Farquhar et al., 2011; Farquhar et al., 2000; Lyons et al., 2014) while some have suggested the rise in O_2 was more gradual and occurred over an extended period of time (Large et al., 2022; Ostrander et al., 2021). This rise in atmospheric O_2 is commonly referred to as the Great Oxidation Event/Episode (GOE; Holland, 2002; Poulton et al., 2021) and is characterised by the disappearance of S-isotope mass independent fractionation (S-MIF) signals in the rock record. Evidence for a major change in the oxidation state of the atmosphere at c. 2.3 Ga was first outlined by Roscoe (1969, 1973) and later refined by Holland (1999), but it was the discovery and confirmation of the variation of S-MIF with time (Farquhar et al., 2000; Holland, 2006; Pavlov and Kasting, 2002) that has led to the adoption of this proxy as the best indicator of the GOE. The S-MIF signal, manifest as non-zero $\Delta^{34}S$ values, is produced in the upper atmosphere via oxygen-free photochemical reactions, and its presence in the multiple sulphur isotope (MSI) record is now widely accepted as a reliable geochemical fingerprint of an anoxic atmosphere. Conversely, the loss of S-MIF between c. 2.45 and 2.30 Ga reflects the development of an oxygenated atmosphere with a $pO_2 < 10^{-5}$ times present atmospheric level (PAL), but its precise timing and tempo are vigorously debated (Bekker et al., 2004; Gumsley et al., 2017; Izon et al., 2022; Philippot et al., 2018; Poulton et al., 2021; Uveges et al., 2023; Warke et al., 2020). Furthermore, while lower limits of O_2 required to remove S-MIF signals from the rock record can be modelled, the uppermost limits are not known. Therefore, the peak of an oxygenation event cannot be derived from the S-MIF technique but only the first rise of atmospheric O_2 (Luo et al., 2016). There are also questions regarding the provenance of the sea water sulphate that preserves the S-MIF signal. It may be possible the signal was developed in the sulphate before being made available as sea water sulphate (Reinhard et al., 2013).

Without necessarily discounting the strong S-MIF signals at c. 2.33 Ga, some studies have suggested there may have been oxygenation events of varying intensities prior to 2.3 Ga (Anbar et al., 2007; Kaufman et al., 2007; Lyons et al., 2014; Ohmoto et al., 2006). These include significantly older Mesoarchean ‘ O_2 oases’ inferred from Mn-enriched BIF and shale in the Pongola and Witwatersrand Supergroups (Albut et al., 2018; Planavsky et al., 2014). Regardless of the nature of the rise of oxygen in the atmosphere–ocean system, the timing, magnitude, and duration of the peak is still controversial. This is problematic especially if the first ever increase in atmospheric O_2 concentrations is expected to help define the APB. Large et al. (2022) attempted to compare several geochemical proxies with other geological records such as temporal trends in black shale and evaporite occurrences (Condie et al., 2001; Golden, 2019), mineral evolution and fossil size (Payne et al., 2009). The main objective was to resolve conflicting interpretations of atmospheric and hydrospheric oxygenation obtained from different geochemical proxies such as variations in redox-sensitive elements (i.e. affected by oxidative weathering) in marine black shales (Mo, U) and sedimentary pyrite (Se, Co, Se/Co), as well as whole-rock isotopes (Cr,

N, C, Mo, S). Despite incomplete records in these proxies, the study concluded that atmospheric O₂ may have gradually increased from around 2700 Ma, peaking around 1900 Ma. These findings were consistent with the various geological records mentioned above. Another similar study by [Ostrander et al. \(2021\)](#) also proposed an increase in oxygen well before the c. 2.33 Ga GOE and that peak O₂ levels were not achieved until well into the Paleoproterozoic.

While understanding that atmosphere-hydrosphere conditions are important, trends in the biosphere can provide useful insights into major changes in geological environments. Undoubtedly, the biosphere has played a role in manipulating atmosphere–ocean redox conditions (including their subsequent manifestations) and continues to do so today. But much of the focus on understanding biosphere evolution is centred around the Ediacaran–Cambrian boundary, owing to the abundance of macroscopic fossils. The APB on the other hand has received very limited attention in comparison, perhaps because the biosphere was microbial and prokaryotic in nature. Additionally, the lack of interest could be attributed to the age of the rocks, metamorphic effects and lack of preservation. [Lepot \(2020\)](#) summarised the origins of various prokaryotic metabolisms and their potential timing, and while pinpointing exact timing proved tricky, the study used bulk-rock geochemistry and petrography to demonstrate that most prokaryotic metabolisms were established by c. 2500 Ma. Another study by [Battistuzzi et al. \(2004\)](#) detailed the prokaryote genomic timescale using molecular clocks (a local clock method) and datasets of amino acid sequences, and also concluded that most metabolic pathways were well established by 2500 Ma with an increased concentration of nodes (branching point in a phylogenetic tree) leading up to this time. However, it should be noted that times of divergence estimates may change with maximum–minimum calibration constraints. For instance, changes in time estimates have been observed when a 2.7 Ga minimum and 2.3 Ga fixed calibration point was changed to 2.3 Ga minimum calibration point. Perhaps the geochemical trends observed in the rock record are a manifestation of a more well-equipped (in terms of cellular machinery) biosphere. Any changes in favour of the biosphere are bound to influence organic matter production and burial, directly impacting oxygen production.

However, there are also some physical criteria, such as glaciogenic diamictites, continental red beds and the presence or absence of redox-sensitive detrital minerals, that either directly or indirectly imply the existence of atmospheric O₂ and hold the most potential for a practical and widely applicable definition of an APB related to the development of an oxidising atmosphere. As discussed below, there is evidence within the MBS for an increase in free O₂ related to a broader GOE that spans both the Hamersley and Turee Creek Groups, although the proxy records are incomplete.

3. The Archean–Proterozoic boundary in Australia

The western two-thirds of the Australian continent preserves an extensive record of Precambrian rocks, developed on three main Archean cratonic nuclei centred on southern, western and northern Australia ([Fig. 1](#)). In the Pilbara region of Western Australia, this record comprises granite-greenstones of the 3800–2830 Ma Pilbara Craton that are overlain along its southern margin by the 2780–2208 Ma Mount Bruce Supergroup (MBS). In stratigraphic order the MBS consists of the 2775–2629 Ma Fortescue Group, the 2629–2420 Ma Hamersley Group and the 2420–2208 Ma Turee Creek Group ([Fig. 1](#)). The Fortescue Group is a 6.5 km-thick volcanic sequence of Archean mafic and felsic volcanic rocks with associated sedimentary units ([Blake, 2001; Thorne and Trendall, 2001](#)) and is conformably overlain by the 3 km thick Hamersley Group, that is composed of extensive banded iron formation (BIF), chert and carbonates, interbedded with siliciclastic and volcanoclastic sedimentary rocks with lesser mafic and felsic igneous rocks ([Kepert, 2018; Trendall and Blockley, 1970](#)). The Hamersley Group spans the Archean–Proterozoic boundary and is paraconformably

overlain by the Turee Creek Group, a siliciclastic succession of approximately 4.5 km thickness interrupted by at least three unconformities and intruded by c. 2208 Ma dolerite sills ([Martin, 2020](#)).

The MBS is a relatively continuous stratigraphic record of the opening and closing of a Neoproterozoic to earliest Paleoproterozoic ocean and marginal sea ([Blake and Barley, 1992](#)) on the southern margin of the Pilbara Craton. The MBS was later deformed during the Paleoproterozoic Ophthalmia Orogeny ([Martin, 2020; Martin et al., 2000; Rasmussen et al., 2005b](#)) along the northern margin of the Capricorn Orogen ([Fig. 1](#)). Significant recent advances have been made in the geological understanding of this region that include lithostratigraphic revisions and identification of new field relationships in the upper part of the MBS, new geochronological and geochemical results throughout the succession, and more detailed understanding of the stratigraphic record of the GOE and associated Huronian glaciations in the Turee Creek Group.

In Western Australia, the chronometric APB is located in the upper Mount McRae Shale of the Hamersley Group ([Fig. 1](#)), based on a multi-sample whole rock Re–Os isochron age of 2501.1 ± 8.2 Ma for samples above a middle marker zone of pyrite nodules ([Anbar et al., 2007](#)), and a SHRIMP zircon ²⁰⁷Pb/²⁰⁶Pb age of 2504 ± 5 Ma of a tuff unit from lower in the formation ([Rasmussen et al., 2005a](#)). A candidate for a GSSP marking the APB that is related to the GOE and associated Huronian Glacial Event (HGE) has been proposed by [Van Kranendonk et al. \(2012\)](#) in the type section of the recently named Cave Hill Member of the Boolgeeda Iron Formation ([Martin, 2020](#)) close to the contact between the Hamersley and Turee Creek Groups ([Fig. 1](#)). Most work relevant to a revised APB in the MBS has focussed on proxies that record the oxidation state of the atmosphere-hydrosphere system, specifically the loss of S-MIF, but the details of related redox-sensitive isotopic and trace element systems, the record of terrestrial red beds and sedimentary manganese and other redox proxies are less well-documented. In this section we summarize significant recent changes to the geological understanding of the MBS that are specifically relevant to considerations of a revised placement of the APB in the vicinity of the contact between the Hamersley and Turee Creek Groups ([Fig. 1](#)), and to definition and naming of the adjacent periods ([Fig. 2](#)).

3.1. Stratigraphic revisions in the Mount Bruce Supergroup

Any proposed change to the placement of the APB, especially one that involves a chronostratigraphic definition tied to the rock record, needs to be cognizant of recent revisions to stratigraphic nomenclature, and important new stratigraphic relationships in the upper part of the MBS ([Martin, 2020](#)). The MBS was originally defined by [Halligan and Daniels \(1964\)](#) and later revised by [Trendall \(1979\)](#), who left several units within the upper-most Turee Creek Group un-named. This situation persisted until [Thorne and Tyler \(1996\)](#) named the Koolbye and Kazput Formations ([Fig. 3](#)), although [Martin et al. \(2000\)](#) later divided the Kazput Formation into informal lower, middle, and upper units. However, usage of the un-named units of [Trendall \(1979\)](#) has persisted (e.g. [Krapež et al., 2017](#)). To aid communication of the geology of this important part of the MBS, all formerly un-named stratigraphic units and significant markers in the Turee Creek Group have now been formalized ([Martin, 2020](#)) and registered in the Australian Stratigraphic Units Database.

There are two critical observations that are relevant to any APB definition related to the GOE. Firstly, the nature of the contact between the Woongarra Rhyolite and the Boolgeeda Iron Formation, which is now considered to be a paraconformity to low-angle unconformity ([Martin, 2020](#)), in contrast to previous interpretations of an intrusive ([Trendall, 1995](#)) or conformable (e.g. [Krapež, 1996; Van Kranendonk et al., 2015b](#)) relationship. This has important implications for the interpretation of geochronological data that might constrain a revised APB. The second important new stratigraphic observation relates to the contact between the Hamersley and Turee Creek Groups, which is

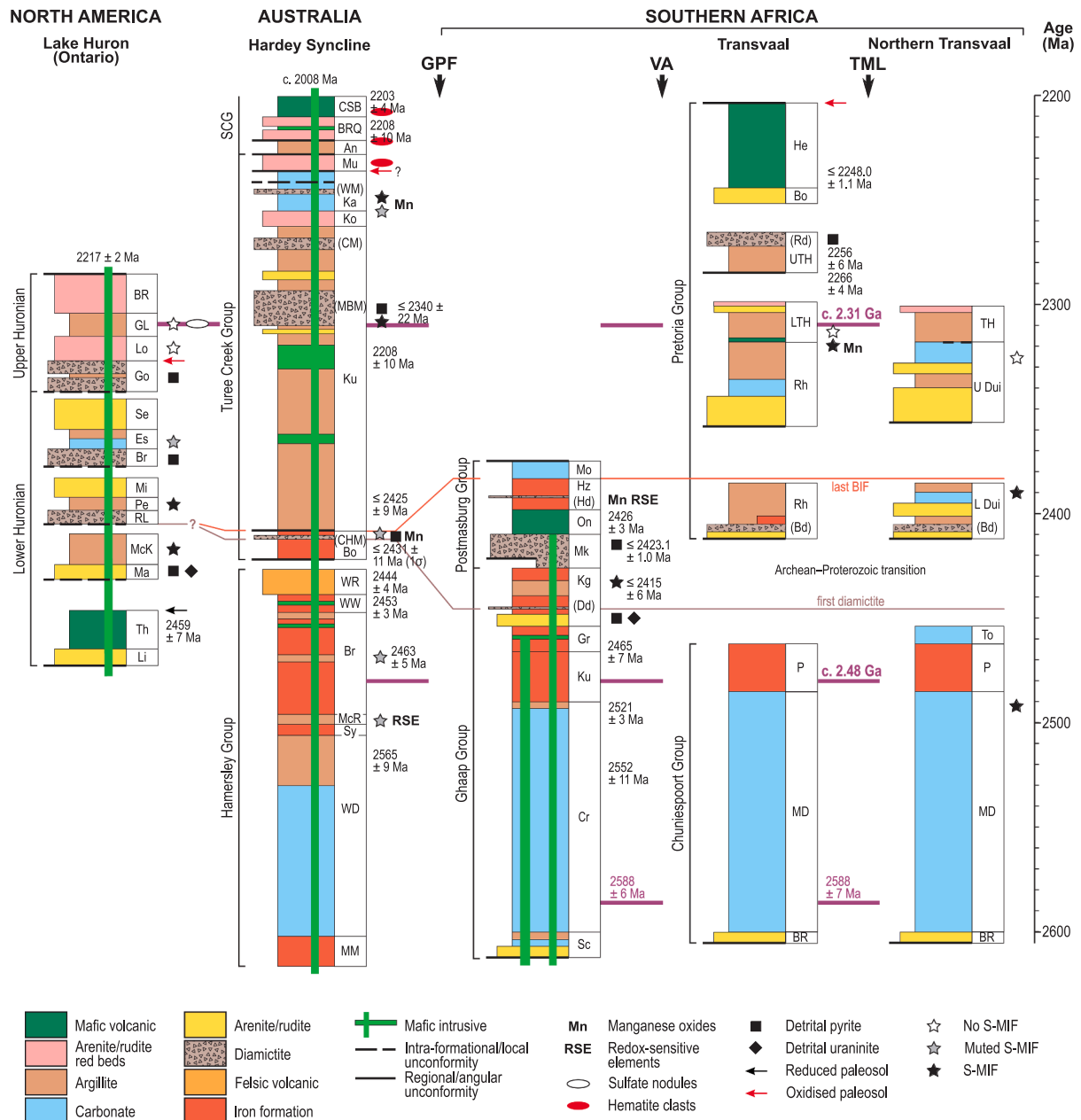


Fig. 3. Proposed global correlation of key stratigraphic records containing candidates for an Archean–Proterozoic GSSP related to the GOE and HGE (see text for discussion and definitions). Modified after Martin and Howard (2023). Stratigraphic columns do not accurately represent either thickness or age, but the sections hang on two well-constrained timelines (purple) that are present in most sections. Huronian Supergroup stratigraphic units (North America): Li = Livingstone Creek Formation, Th = Thessalon Formation, Ma = Matinenda Formation, McK = McKim Formation, RL = Ramsay Lake Formation, Pe = Pecors Formation, Mi = Mississagi Formation, Br = Bruce Formation, Es = Espanola Formation, Se = Serpent Formation, Lo = Lorrain Formation, GL = Gordon Lake Formation, BR = Bar River Formation. Mount Bruce Supergroup stratigraphic units (Australia): MM = Marra Mamba Iron Formation, WD = Wittenoom Dolomite, Sy = Mount Sylvia Formation, McR = Mount McRae Shale, Br = Brockman Iron Formation, WW = Weeli Wolli Iron Formation, WR = Woongarra Rhyolite, Bo = Boolgeeda Iron Formation, (CHM) = Cave Hill Member, Ku = Kungarra Formation, (MBM) = Meteorite Bore Member, (CM) = Calgra Member, Ko = Koolbye Formation, Ka = Kazput Formation, (WM) = Wonangara Member, Mu = Munder Formation, An = Anthiby Formation, BRQ = Beasley River Quartzite, CSB = Cheela Springs Basalt. SCG = Shingle Creek Group. Transvaal Supergroup stratigraphic units (Southern Africa): Griquatown West stratigraphic units: Sc = Schmidtsdrift Subgroup, Ku = Kuruman Iron Formation, Gr = Griquatown Iron Formation, Kg = Koegas Subgroup, (Dd) = Doradale diamictite, Mk = Makganyene Formation, On = Ongeluk Formation, Hz = Hotazel Formation, (Hd) = Hotazel diamictite, Mo = Mooidraai Formation. Note the two lesser known diamictites in this region, below and above the Makganyene Formation (Polteau et al., 2006). Transvaal stratigraphic units: BR = Black Reef Formation, MD = Malmani Dolomite, P = Penge Formation, Rh = Rooihooft Formation, (Bd) = Bewaarkloof diamictite, LTH = lower Timeball Hill Formation, UTH = upper Timeball Hill Formation, (Rd) = Rietfontein diamictite, Bo = Boshoeck Formation, He = Hekpoort Formation. Northern Transvaal stratigraphic units: BR = Black Reef Formation, MD = Malmani Dolomite, P = Penge Formation, To = Tongwane Formation, L Dui = lower Duitschland Formation, U Dui = upper Duitschland Formation, TH = Timeball Hill Formation. OG = Olifantshoek Group. Units in parentheses are informal or member-level units. Outcrop areas in Southern Africa are separated by two distinct structural features, the Vryburg Arch (VA) and Thabazimbi–Murchison Lineament (TML). The Griquatown–Poonda Fault (GPF) marks the relative position of the faults interpreted to separate platform and basal facies in the Chuniespoort/Ghaap and Hamersley Groups respectively and are commonly considered as strike equivalents within a Vaalbara reconstruction (Fig. 4). A revised Archean–Proterozoic transition is also shown, bound by the first appearance of glaciogenic diamictite and last occurrence of Superior-style platform BIF. (For interpretation of the references to colour in this figure legend, the reader is referred to the web version of this article.)

generally paraconformable but locally weakly angular (Martin, 2020). This will have important implications for selecting a GSSP for a revised APB at this stratigraphic level, especially if such diastems are to be avoided in the selection of a boundary (Salvador, 1994). An additional problem relates to the identification of bed-level erosional surfaces in the uppermost Boolgeeda Iron Formation (Martin, 2020) where a revised APB might be placed.

3.2. Changing tectonic style

Early debates surrounding recognition and definition of an APB were centred on the interpretation that this boundary could be defined in terms of a diachronous transition related to a change in tectonic style (e.g. Windley, 1984). The Archean was primarily thought to be characterized by highly deformed granite-greenstone belts, whereas the Proterozoic was characterized by relatively undeformed platform cover that unconformably overlies successions of demonstrably 'Archean' character. The 2500 Ma chronometric boundary was therefore chosen such that it delimits the Archean, rather than defining it (Plumb and James, 1986). Gradstein et al. (2004) later proposed an Archean-Proterozoic transition from 2600 to 2300 Ma defined by the onset of giant BIF deposition and terminated by the first appearance of continental red beds. In the MBS this age range equates chronologically to the Hamersley Group and the bulk of the Turee Creek Group. However, as highlighted by Trendall (1984), there is no evidence for any transition related to the chronometric APB in Australia or Southern Africa. The change in tectonic style as originally envisaged occurs much earlier in Australia, (c. 2780 Ma as represented by the unconformity at the base of the Fortescue Group; Trendall, 1984). Subduction-like signatures are observed in the early evolution of the Pilbara Craton (Hickman, 2004; Hickman and Van Kranendonk, 2012; Van Kranendonk et al., 2007); however, their origins remain debated and this does not necessitate horizontal tectonics being active (e.g. Gardiner et al., 2017; Johnson et al., 2017). Locally, some form of vertical tectonics was active at least until late into the deposition of the Fortescue Group (Van Kranendonk, 2003), and possibly later as reflected in the "Rocklean movement" of Kepert (2018). A global plate tectonic shut down has also been proposed during the Paleoproterozoic (e.g. Pehrsson et al., 2014; Spencer et al., 2018) although this is not particularly evident in the MBS (e.g. Barley et al., 1997; Blake and Barley, 1992). Changing tectonic style is therefore not a good basis for defining the APB on the Pilbara Craton or globally.

However, differences in interpretation of tectonic setting, particularly of the Turee Creek Group, and the timing of orogenesis (e.g. Krapež et al., 2017; Van Kranendonk et al., 2015b) have strongly influenced the most recent attempt at global stratigraphic correlation of the main relevant successions (Bekker et al., 2020). Whilst the geological basis for some of these interpretations has since been questioned, their resolution is beyond the scope of this contribution, and the reader is referred to Mazumder (2017), Philippot et al. (2021) and Martin (2020) for a consideration of the issues. Correct interpretation of these aspects of local geology are critical for the interpretation and global correlation of the proxy records on which a revised APB definition will rely.

3.3. Sulfur isotopes

There is a growing consensus reflected in the proposals of Van Kranendonk et al. (2012) and Shields et al. (2022) to re-define the APB based on recognition of the GOE and related diamictites deposited during the HGE. However, some of the key sticking points in this debate surrounding recognition of the GOE relate to the age constraints and regional to global correlation of critical S-isotope records (e.g. Bekker et al., 2020; Gumsley et al., 2017), the significance of recycling of S-MIF sulfides to produce what has been termed the crustal memory effect (CME; e.g. Philippot et al., 2018; Reinhard et al., 2013; Uveges et al., 2023), and spatial, temporal, and lithological biases in the global MSI

database (Uveges et al., 2023). Recently, Uveges et al. (2023) attempted to address some of these issues and demonstrated that the global expression of the CME is barely detectable, and that rare post-2.3 Ga instances of S-MIF are ephemeral and operated on sub- 10^4 yr timescales. The MSI record of the MBS is fragmentary, with very little data in the immediate aftermath of the controversial 'whiff of oxygen' in the Mount McRae Shale (Anbar et al., 2007; Slotznick et al., 2022) and a transient S-MIF event in the basal Kazput Formation (Killingsworth et al., 2019; Philippot et al., 2018; Uveges et al., 2023). Global correlation of this fragmentary record is hampered by the persistence of a muted S-MIF signal in the Turee Creek Group (Fig. 3) that is interpreted to reflect the interplay between a weathering-derived component and a lithological control (Uveges et al., 2023). Also, despite the best efforts of Uveges et al. (2023) there are still biases and errors in the MSI database that can only be addressed with new sampling and geological studies. The MBS presents a unique opportunity in this regard in that it is a coherent and mostly conformable stratigraphic succession with relatively good geochronological constraints.

A detailed investigation of S-isotopes in the Mount McRae Shale (MMS) was carried out by Williford et al. (2016) and special consideration was given to identifying the S-MIF signals and explaining the observed S-isotope compositions of whole rock and precise in-situ pyrite analyses. The study noted large heterogeneities in S-isotope compositions and that the production and preservation of S-MIF in the MMS may be dependent on a variety of local factors. These include pore fluid S-isotope chemistry, changes in S-MIF with regards to growth of a particular texture (nodule), and metabolic recycling of S which may render high $\Delta^{33}\text{S}$ in a closed system. There is comparatively little S-isotope data above the MMS in the Hamersley Group. S-isotope compositions in some samples from Slotznick et al. (2022) suggested that S-isotope systematics do not necessarily show temporal trends but are a product of processes such as later fluid flow or recrystallisation. A range of $\Delta^{33}\text{S}$ values were observed in the different textures of pyrite with early pyrites carrying negative $\Delta^{33}\text{S}$ and the opposite for late pyrite textures. This reinforces a point made by Gregory et al. (2019) that only nodules that have grown via a pervasive growth mechanism involving multiple nucleation sites, that results in chemical homogeneity across the nodule and a lack of trace element and isotopic zonation, can be reliably used for interpreting past marine conditions.

3.4. Glacigenic diamictites

Perhaps the most important new stratigraphic observation is the recognition of four diamictite intervals in the upper MBS, which have each been formally named at member level and described in detail to improve geological communication (Martin, 2020). It is important to note that all diamictites described in this paper are identified independently of interpretations of depositional environment, although each displays some evidence of the action of glacigenic processes. The lowermost diamictite-bearing horizon of the MBS, the Cave Hill Member, represents the uppermost 10 m of the Boolgeeda Iron Formation in areas where it has not been eroded beneath the paraconformity at the base of the Kungarra Formation of the Turee Creek Group. The diamictite component forms the base of the member and is usually no more than a few decimetres thick. It is also the diamictite with the most convincing evidence for ice-rafted deposition (Martin, 1999; Van Kranendonk et al., 2015b), although its glacial interpretation has recently been questioned (Bekker et al., 2020). The second diamictite is the well-known Meteorite Bore Member of the Kungarra Formation that was named by Trendall (1979), and incorrectly correlated with the Cave Hill Member by Martin (1999). For the sake of clarity of communication and because it is about 500 m above the Meteorite Bore Member (Fig. 3), and stratigraphically distinct, the third diamictite has been named the Calgra Member. This diamictite was first explicitly recognized but not named by Martin and Morris (2010) and Van Kranendonk et al. (2015), although Krapež et al. (2017) included it in their depiction of the

Meteorite Bore Member. It is apparent from his description of the Meteorite Bore Member that Trendall (1979) was also not aware of the existence of the Calgra Member. The fourth diamictite is in the lower part of a fine-grained siliciclastic unit within the Kazput Formation that has been named the Wonangara Member (Martin, 2020). The diamictite in the Wonangara Member is characterized by faceted clasts that are like those in the other diamictites, but due to the effects of weathering and the discontinuity of outcrops its glacial origin is the least certain. However, the recognition of potentially up to four stratigraphically discrete Paleoproterozoic diamictite horizons within a relatively coherent stratigraphic succession has important implications for global correlations that will be discussed later.

3.5. Redox chemistry and other isotopes

Chemostratigraphy provides a powerful tool for studying the GOE and establishing any potential APB (e.g. Gaucher and Frei, 2018; Kendall, 2021), although the proxies used mainly track oxygenation of the hydrosphere rather than the atmosphere. Whole rock and pyrite geochemistry of the MMS were investigated by Gregory et al. (2015). Both techniques yielded similar results, that show enriched concentrations of redox sensitive trace elements such as Mo, Co, Cr, Cu and Zn in the upper MMS. The enrichment typifies an intense oxygenation event, which was also previously identified by Anbar et al. (2007). High Fe/Al ratios were also observed during the deposition of the MMS implying higher Fe²⁺ availability in the oceans. The lower part of the MMS is believed to have been deposited under relatively lower Fe²⁺ conditions compared to the upper part. Such variations may lead to opposite trends in geochemical signals in whole rock versus pyrite during oxygenation events. For instance, elements such as Ni, Co, Cu, Te, Au and Ag show whole-rock enrichment in the MMS compared to pyrite geochemistry. Gregory et al. (2015) attributed that enrichment to higher concentrations of sulphate in the oceans due to oxidative weathering on land in an Fe²⁺ enriched ocean. Rocks with a higher degree of pyritization (>10 % pyrite) impart an imbalance in trace metal partitioning in whole rock and pyrite. Overall, the study revealed that the enrichment of redox sensitive trace elements in the MMS was higher than all other sequences in the MBS.

Novel geochemical proxies provide additional evidence for redox processes occurring in the lead up to the GOE, with numerous studies suggesting that transient periods of enhanced O₂ occurred before the main GOE (Anbar et al., 2007; Kurzweil et al., 2015; Wille et al., 2007). Redox sensitive elements are the most promising archives with Cr, Mo and U isotopes all showing significant excursions, which have been interpreted to be the result of atmospheric or oceanic oxygenation (Árting et al., 2023; Brüske et al., 2020; Frei et al., 2009; Kendall et al., 2015; Koehler et al., 2018; Kurzweil et al., 2015). While other redox sensitive elements such as Cu contemporaneously display limited fluctuations over the period of interest (Thibon et al., 2019) highlighting the complexity of interpretation of these records.

Recently, Slotznick et al. (2022) presented refined arguments against evidence for oxygenation during the deposition of the MMS. The study used a variety of in-situ analytical techniques to carefully explain and argue against all previous enrichments normally attributed to higher atmospheric O₂. For instance, enriched Mo and organic matter in the MMS would normally be considered a consequence of higher atmospheric O₂. However, Slotznick et al. (2022) explained higher Mo concentrations in the pyrite were originally sourced from volcanic glass, and that later dissolution of the glass and remobilisation of Mo caused the high values. While this may be a plausible explanation of Mo enrichment in the rocks, it doesn't explain the higher concentration of redox sensitive trace elements in the MMS (see also Anbar et al., 2023). Likewise high concentrations of organic matter would normally imply high organic carbon burial, and by extension higher O₂ release due to the burial of C_{org}. Slotznick et al. (2022) interpret higher C_{org} accumulation in the MMS as the product of extremely slow sedimentation rates in an

anoxic environment as opposed to high rates of organic matter productivity. It is true that lower sedimentation rates coupled with lower O₂ may cause higher organic matter preservation, but if a rise from 5 % to 15 % total C_{org} in the samples is not due to an increase in C_{org} productivity, there can be two other possibilities. Either C_{org} production remained the same and O₂ exposure continued to decline, or C_{org} productivity did increase but at a lower rate than apparent (5 to 15 %). The former implies higher O₂ concentration before the 'whiff', which is unlikely. Also unlikely is that C_{org} production remained the same for 50 million years. The latter may be more plausible, where organic matter productivity did increase but there wasn't enough O₂ to decompose organic matter, hence causing higher preservation. Either way, the MMS is a more carbonaceous unit compared to under- and overlying formations.

Widespread Mn precipitation such as that observed in the Mn-rich horizons in southern Africa (Kirschvink et al., 2000; Warke et al., 2020), requires large quantities of O₂ at c. 2.4 Ga to facilitate shallow-water Mn precipitation (e.g. Robbins et al., 2023), although this requirement is disputed by Johnson et al. (2013). The observation of distinct light U isotope compositions in similar Southern African horizons has been explained by the onset of partial U mobilization during slow oxidative weathering of uraninite shortly before and during the GOE (Brüske et al., 2020). Turning specifically to the Australian stratigraphic record, the MMS preserves several key indicators of increased oxygenation prior to the GOE characterised by positive Mo, U and Se isotope excursions (Anbar et al., 2007; Kendall et al., 2015; Stüeken et al., 2015) and oxidative mobilization of Mo, Os and Re (Kendall et al., 2015). Steadman et al. (2020) inferred a c. 2–10 % rise in O₂ concentrations, derived using Se/Co values in sedimentary pyrite, moving up stratigraphy in the MMS, although this observation was based on an extremely limited sample set. Lantink et al. (2023) have recently identified sharp enrichments of redox sensitive elements in the Joffre Member of the Brockman Iron Formation prior to the GOE that have been interpreted as diagenetic redox fronts formed in response to precessional Milankovitch forcing. Overall, evidence from geochemical proxies of oxidation at present remains limited from throughout the MBS and further work is required to complete the record.

Closely associated with the GOE are two positive carbonate carbon isotope excursions ($\delta^{13}\text{C}_{\text{carb}}$) that each follow closely after a glacial event (Bekker et al., 2006). The origin and significance of these excursions to the GOE are complex and debated, but the simplest interpretation is that they reflect the burial of organic carbon that in turn allowed further accumulation of atmospheric O₂ (Fakhræe et al., 2023; Martin et al., 2013; Prave et al., 2022). The oldest of these is only recorded in South Africa and has been named the Deutschland event (Bekker et al., 2001), but the younger event is more widespread and has been used for global correlations (Bekker et al., 2020). This second event is known as the Lomagundi event, but so far neither event has been recognised in the Australian record. This is almost certainly a function of incomplete sampling and the absence of carbonates at the correct stratigraphic level. The first comprehensive C-isotope record for Australia was compiled by Lindsay and Brasier (2002), and later expanded by Martindale et al. (2015) who also corrected some stratigraphic errors in the original compilation. However, there is a significant interval of carbonate above the K2 section of Martindale et al. (2015) in the upper Kazput Formation that is above the Wonangara Member and has not been analysed for carbon isotopes, probably because they misinterpreted the extent of the Beasley River Quartzite (see Martin, 2020). There are also several unanalysed carbonate horizons, some of which are stromatolitic, that cap shallowing-upward progradational cycles below the Meteorite Bore Member, and in the section between the Calgra Member and the Koolbye Formation. Outcrop is poor in the main area of exposure, the Hardey Syncline (Martin, 2020), and reliable expansion of any isotopic records across this interval will likely require more targeted stratigraphic drilling.

3.6. Physical proxies of oxidation state

The MBS (and Turee Creek Group in particular) records several physical proxies of atmospheric oxidation state that are presently poorly documented in Australia, but may provide a complementary but more practical means to identify global GOE-related successions (Cloud, 1976, 1972; Holland, 1999) compared to the isotopic and geochemical proxies used to recognise the GOE discussed above. The earliest and longest ranging of these proxies is the detrital pyrite and uraninite record presented by Bekker et al., (2020, Fig. 2), which extends from the middle Boolgeeda Iron Formation to the Anthiby Formation. However, this record differs from previous pyrite studies (Philippot et al., 2018), and no verifiable data was presented or referenced for the presence of uraninite, or the full expanded stratigraphic range of detrital pyrite (not shown in Fig. 3).

Instead, perhaps the most useful of the physical proxies is the presence of terrestrial red beds with hematite cements (Cloud, 1976; Holland, 1999) that make their first appearance in tidal facies of the Koolbye Formation (Mazumder et al., 2015), but are also present in fluvial facies of the Munder Formation and basal units of the overlying Wyloo Group (Fig. 1). In addition to hematite cements in sandstones, conglomerates with microplaty hematite ore-clasts and hematite cements have recently been discovered at the base of the Munder Formation (Martin, 2020), further expanding the style and stratigraphic range of terrestrial red bed sedimentary rocks in the TCG. Another relevant potential indicator of marine redox conditions is the presence of small manganese oxide nodules in dolomites of the lower Kazput Formation (see fig. 31 in Martin and Howard, 2023). These nodules appear to be primary features but may reflect modern weathering of Mn-rich carbonates. However, they also coincide with the transient S-MIF values in the lower Kazput Formation (Fig. 3). Mn-rich ferruginous mudstones are also known from the top of the Calgra Member (Van Kranendonk et al., 2012; Van Kranendonk and Mazumder, 2015). Further study of these physical proxies in the MBS and their significance to the delineation of the GOE in the stratigraphic record is required. Oxidised paleosols (Rye and Holland, 1998) are also closely correlated with the presence of red beds in many successions containing the GOE, and a potential example underlies the unconformity at the base of the Munder Formation (Fig. 3; Martin, 2020). However, it is not yet clear whether this is a more recent weathering effect, and confirmation of its deep-time origins as suggested by karst dissolution of the Kazput Formation will require fresh sample material.

3.7. Geochronology

In addition to the stratigraphic revisions described above, recent work has also significantly improved the geochronological constraints on the MBS, compared to the seminal work of Trendall et al. (2004). This has involved re-analysis of some of the key intervals, new data from critical parts of the stratigraphy, and a re-evaluation of the stratigraphic context of some existing dates. Accurate geochronological constraints are critical for reliable time-series analysis of datasets such as the MSI database (e.g. Uveges et al., 2023) that underpins the definition of the GOE, and for global chronostratigraphic correlation. Geochronology also supports the revised interpretations of stratigraphic relationships at the contact between the Hamersley and Turee Creek Groups. Only the most significant dates will be considered here; more detailed accounts of the revisions are available in Martin (2020) and Martin and Howard (2023).

The presence of the chronometric APB within the Mount McRae Shale (MMS) is well constrained by published data and is supported by new ages from the base of the Brockman Iron Formation of the MBS (see fig. 7 in Martin and Howard, 2023). Rasmussen et al. (2005) did not report the exact stratigraphic location of the 2504 ± 5 Ma tuff bed that they dated in the MMS. The lithological description of the sample, combined with known stratigraphic variations, suggests that it comes

from the lower two thirds of the MMS. This interpretation is corroborated by a well-located Re–Os isochron of 2501.1 ± 8.2 Ma from the S1 subdivision in the upper half of the formation (Anbar et al., 2007). New ages for the two lowermost shale macrobands in the Brockman Iron Formation of 2485 ± 9 Ma (Wingate et al., 2021a) and 2480 ± 7 Ma (Wingate et al., 2021b) can be used to estimate a compacted depositional rate for the intervening 6 m-thick BIF macroband that is between 0.3 and 2 m/my (mean 1.2 m/my), which is significantly slower than previous estimates from the Brockman Iron Formation (Lantink et al., 2022; Rodrigues, P. de O. C. et al., 2019; Trendall et al., 2004). Numerous factors can account for these discrepancies including real changes with time, different age constraints or thicknesses used in calculations, differences in depositional rate for different lithologies, and a lack of well-constrained depositional rates for non-BIF lithologies in the Hamersley Group. Nonetheless, application of this new depositional rate for the lower Brockman Iron Formation BIF, confirms the 2494 Ma interpolated age for the base of the formation (Trendall et al., 2004).

Slotznick et al. (2022) presented new geochronological data that suggest that the lower MMS is significantly older (2533 ± 6 Ma) than the interpolated 2505 Ma maximum age of Trendall et al. (2004), and that the depositional rate of shale (1.03 to 1.76 m/my) is almost identical to that calculated here for BIF. However, their rate calculation relies on correlation between two drillholes (APDP9 and WLT10), the details of which were not presented, and photomicrographs of the dated zircon grains suggest from their shape that they may be detrital. If the ages of Slotznick et al. (2022) are indeed magmatic, then this implies that the ages used to calculate the BIF depositional rate described above are likely detrital, and the rate calculations spurious. Resolution of such discrepancies in the geochronological record and its interpretation are imperative to any efforts to radiometrically constrain the APB, regardless of where it is placed.

Revised stratigraphic relationships in the uppermost Hamersley Group have significant implications for interpreting geochronological data related to the proposed APB of Van Kranendonk et al. (2012), or any potential alternatives, because the 2445 ± 5 Ma tuff bed dated by Trendall et al. (2004) and interpreted to constrain igneous crystallization of the uppermost Woongarra Rhyolite is now considered to be a maximum depositional age for the basal Boolgeeda Iron Formation (Martin, 2020). This interpretation is supported by a maximum depositional age of 2442 ± 8 Ma (Wingate et al., 2020) from the same interval approximately 100 km southeast of Trendall's locality, and an igneous crystallization age of 2444 ± 4 Ma (Wingate et al., 2018a) within the uppermost Woongarra Rhyolite. These ages, combined with the presence of demonstrable Woongarra Rhyolite clasts in the Cave Hill Member (Martin, 1999) indicate a significant hiatus at the base of the redefined Boolgeeda Iron Formation during which the Hamersley Group was uplifted and eroded south of the present outcrop area (Martin, 2020). Consequently, zircon grains older than c. 2.44 Ga dominate the detrital record in overlying units, which complicates meaningful interpretation of the geochronological record and estimation of the age of the APB proposed by Van Kranendonk et al. (2012). However, younger detrital zircon grains ranging from c. 2420–2340 Ma (Caquineau et al., 2018; Takehara et al., 2010; Wingate et al., 2018b) are present in samples above this hiatus and support the interpretation that the Boolgeeda Iron Formation and Kungarra Formation are possibly significantly younger than c. 2425 Ma (Martin, 2020). More detailed geochronological studies around the contact between these two formations are required to further refine estimates of the age of a revised APB, and for improved global correlation.

4. Global correlations

Ratification of a chronostratigraphic definition of the APB, based on recognition of the proxy record of the GOE, will require demonstration of its global applicability. We propose that the MBS is the most appropriate succession in which to define the associated GSSP, primarily

because of its well-preserved coherent stratigraphic record that can be readily correlated with other regions that preserve the GOE. However, these correlations are not without their uncertainties and controversies, which are largely based on data gaps or misinterpretations of local geology. Here we present some important updates regarding the MBS that have implications for resolving global correlation issues. The three most important areas for global correlation that will be discussed here are North America, Southern Africa, and Fennoscandia. West Africa is also emerging as a key area with potential for resolving the finer details of the MSI record and trajectory of the GOE (e.g. Canfield et al., 2013; Paiste et al., 2020), and India will likely also be important (e.g. Mazumder et al., 2019), but these areas will not be considered further here. The proxy records in each of the regions under consideration, particularly S-isotopes, are incomplete and difficult to reconcile with each other, mainly due to poor age constraints, unresolved correlations, and facies dependencies; these discrepancies have strongly influenced previous attempts at global correlation and interpretation of the GOE (e.g. Bekker et al., 2020; Philippot et al., 2018; Izon et al., 2022).

Another important consideration that has not been adequately addressed in previous correlations of the GOE is the tectonic and paleogeographic setting of each region at that time. This is particularly important when comparing Western Australia and Southern Africa where depositional and tectonic polarities strongly determine the permissible correlations (Figs. 3 and 4) within the well-established Vaalbara cratonic reconstruction (Cheney, 1996; de Kock et al., 2009; Wingate, 1998). Such reconstructions are also generally not factored into the correlation of geochemical and isotopic proxy records that are increasingly being shown to have strong local or facies controls (e.g. Molén, 2024; Paiste et al., 2020; Pasquier et al., 2021; Prave et al., 2022; Uveges et al., 2023; Warke et al., 2020; Warke and Schröder, 2018). The correlations presented here are also strongly dependent on two robust geochronological timelines that tie most sections (Fig. 3), pinning pre-GOE strata at c. 2.48 Ga and syn- to post-GOE strata at c. 2.31 Ga (after Philippot et al., 2018; Rasmussen et al., 2013). These tie-lines, combined with the latest geochronology, proxy data and stratigraphic correlations, permit a revised global correlation of the key stratigraphic

records associated with the GOE that has important implications for defining an associated chronostratigraphic APB.

4.1. Southern Africa

The Transvaal Supergroup of Southern Africa (Fig. 3) comprises a comparable stratigraphic record to the MBS with which it has been correlated in detail in many studies (e.g. Bekker et al., 2020; Beukes and Gutzmer, 2008; Martin et al., 1998; Nelson et al., 1999). Despite many units having well-established correlatives in Western Australia as part of the Paleoproterozoic Vaalbara supercraton (Cheney, 1996; Wingate, 1998; de Kock et al., 2009), it is the uncertainties in regional correlations within Southern Africa that bias global correlations and have been largely responsible for interpretations of a staged or oscillatory GOE. However, despite these uncertainties, the Transvaal Supergroup has been the primary focus of recent efforts to decipher the timing and trajectory of the GOE (e.g. Gumsley et al., 2017; Bekker et al., 2020). The bulk of the MSI data that underpins interpretations of the GOE in Southern Africa come from the Pretoria Group (Fig. 3), where the uppermost Rooihooft Formation preserves the youngest known S-MIF signal characterized by high positive $\Delta^{33}\text{S}$ values that constrain this event to c. 2.3 Ga (Rasmussen et al., 2013; Luo et al., 2016; Uveges et al., 2023). However, Schier et al. (2020) used various geochemical proxies to infer oxidative weathering and seawater conditions during earlier deposition of the Hotazel Formation (Fig. 3), although iron isotope data from the same unit have been used to infer that the GOE is not recorded at this level in the Griqualand West region (Lantink et al., 2018). Post-GOE elevated S-MIF in the Timeball Hill Formation is likely short lived and interpreted to be the product of a sensitive atmospheric state that was susceptible to perturbation as O_2 contents varied (Uveges et al., 2023).

Stratigraphic correlations within the Transvaal Supergroup are hampered by facies changes and faulting in the Griqualand West region, lack of outcrop continuity across the Vryburg Arch (Fig. 4), and facies changes across a major basin-bounding fault known as the Thabazimbi-Murchison Lineament (TML; Clendenin, 1989; Clendenin et al., 1988;

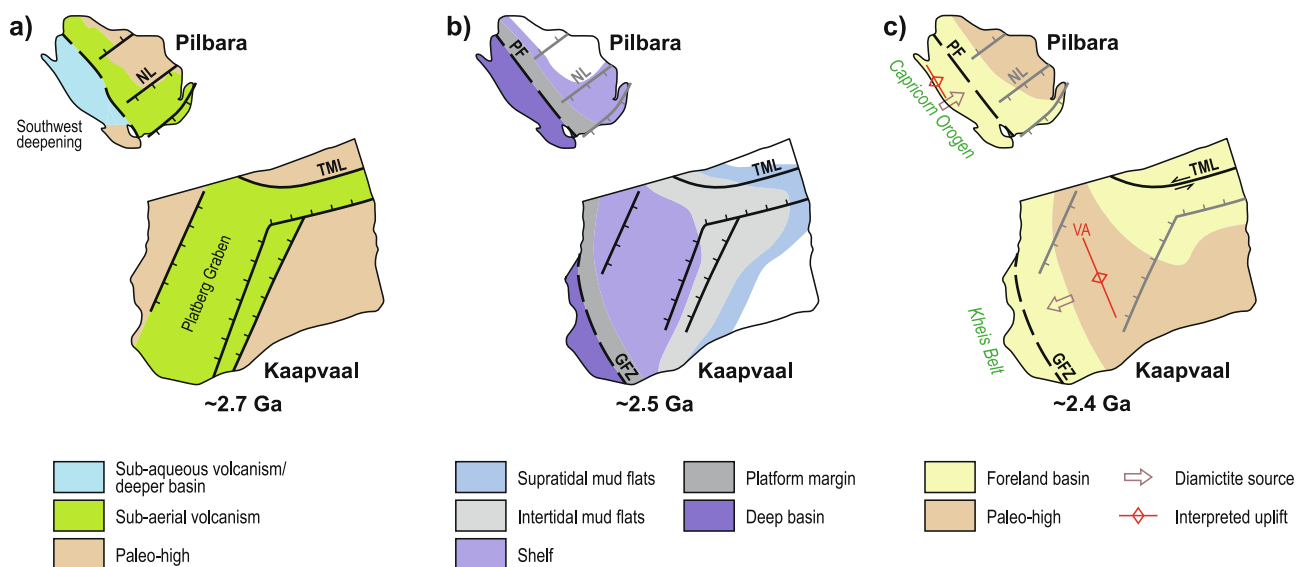


Fig. 4. Schematic paleogeographic reconstruction of the Pilbara (P) and Kaapvaal (K) Cratons in a Vaalbara configuration: a) structural architecture and depositional setting of the Fortescue Group (P) and Ventersdorp Supergroup (K) during intracratonic rifting events that establish the relative positions of the cratons at c. 2.7 Ga (after de Kock et al., 2009); b) basin architecture during deposition of the Hamersley (P) and Chuniespoort/Ghaap (K) Groups at c. 2.5 Ga (after Beukes and Gutzmer, 2008; Clendenin, 1989); c) interpreted paleogeography based on structural and depositional asymmetries related to the Turee Creek (P) and Postmasburg/Olifantshoek/Pretoria (K) Groups, and their adjacent orogenic belts (green text). Basin-margin structures on the Pilbara Craton after Blake (2001) and Thorne and Trendall (2001); Kaapvaal Craton after Clendenin et al. (1988). Active or bounding structures in black, passive structures in grey. NL = Nullagine Lineament; TML = Thabazimbi-Murchison Lineament; PF = Poonda Fault; GFZ = Griquatown Fault zone; VA = Vryburg Arch. (For interpretation of the references to colour in this figure legend, the reader is referred to the web version of this article.)

Martin et al., 1998; Martin, 1990). Correlations in pre-GOE strata comprising the Chuniespoort and Ghaap Groups (Fig. 3) are well established based on lithostratigraphy, sequence stratigraphy, and geochronology (Beukes and Gutzmer, 2008; Clendenin, 1989; Martin et al., 1998; Nelson et al., 1999). However, correlation within the Pretoria Group is more problematic, as is its relationship with the Postmasburg Group (Polteau, 2005). Early lithostratigraphic correlations relied on an interpreted equivalence between the Ongeluk and Hekpoort Formations (e.g. Beukes and Gutzmer, 2008) until the former was shown by Gumsley et al. (2017) to be significantly older than the latter (Fig. 3). A significant consequence of the Gumsley et al. (2017) correlation was the recognition that the Southern African stratigraphic record contains at least three Paleoproterozoic glacial diamictites, although other lesser known diamictites were not considered.

In the Griqualand West region, the main diamictite-bearing interval is the Makganyene Formation that also comprises shale, sandstone, BIF and stromatolitic carbonate, and is gradationally overlain by basalts of the c. 2424 Ma Ongeluk Formation (e.g. Polteau et al., 2006). However, diamictite has also been identified in the Doradale Formation at the base of the Koegas Subgroup, and at the gradational contact between the Hotazel and Ongeluk Formations in the lower Postmasburg Group (Fig. 3; Polteau et al., 2006; Polteau, 2005). Field relationships also indicate that the Makganyene Formation unconformably overlies the Ashesheuwels Subgroup east of the Griquatown Fault zone and conformably overlies the Koegas Subgroup to the west (Ngobeli, 2019; Polteau, 2005). Based on current constraints, the Makganyene Formation has no correlative in the Pretoria Group to the northeast of the Vryburg Arch, but two younger diamictites are recognised in the basal Rooihooft/Duitschland and upper Timeball Hill Formations (Fig. 3). These are informally known as the Bewaarkloof (Havsteen et al., 2023) and Rietfontein (Dorland, 1999) diamictites respectively, although Martini (1979) recognized several diamictites in the Duitschland Formation. However, in the absence of precise age constraints on the lower Rooihooft/Duitschland Formations, combined with the local presence of the Jwaneng Iron Formation (Havsteen et al., 2023) in the Rooihooft Formation (Fig. 3), a correlation between the Bewaarkloof and Makganyene diamictites cannot be ruled out. Altogether these observations do not support direct correlation of any of these diamictites with supposed equivalents in the MBS, nor interpretations of widespread low latitude deposition under 'snowball Earth' conditions (cf. Bekker et al., 2020; Evans et al., 1997; Kirschvink et al., 2000; Young, 2019).

Uncertainties regarding the relationship between the Rooihooft and Duitschland Formations across the TML have been central to the debate surrounding the timing and trajectory of the GOE. In the main outcrop area of the Pretoria Group, to the south of the TML, the Timeball Hill Formation conformably overlies the Rooihooft Formation whereas to the north of this structure it conformably to locally unconformably overlies the Duitschland Formation (Fig. 3). Some studies have treated the Rooihooft and Duitschland Formations as temporally separate entities (e.g. Bekker et al., 2020; Catuneanu and Eriksson, 2002; Gumsley et al., 2017; Humbert et al., 2018), whereas others have correlated them (e.g. Coetzee, 2001; Dorland, 1999; Luo et al., 2016; Warke et al., 2018; Warke and Schröder, 2018). The latter interpretation has most recently been confirmed by Havsteen et al. (2023) and is supported here.

All lithostratigraphic correlations are further complicated by well-documented unconformities or depositional hiatuses that specifically complicate correlation of the diamictites but are also not straightforward themselves due to lack of continuity of outcrop. In the absence of geochronological constraints on the Duitschland Formation, the precise correlation of the mid-Timeball Hill and mid-Duitschland unconformities remain uncertain (Fig. 3). Depending on how the Southern African unconformities are correlated, there could be between five and seven diamictite horizons related to the GOE, excluding a potential additional fluvio-glacial conglomerate in the Boshhoek Formation (Humbert et al., 2018). Resolution of these correlation issues awaits

further work, but the relatively conformable equivalent interval in the MBS provides a template against which to compare.

Any correlation between the West Australian and Southern African stratigraphic records must also consider the relative paleogeographic location, tectonic setting, and depositional polarity of these two regions at the time of the GOE. Paleomagnetic constraints are sparse with limited temporal overlap between regions (Wingate, 1998; de Kock et al., 2009; Evans et al., 1997), but when combined with other geological data suggest that the Pilbara Craton was located to the northwest of the Kaapvaal Craton in present-day coordinates, probably along a contiguous margin (Martin et al., 1998). Within this framework, the geological data suggest that the bulk of the pre-GOE stratigraphic record in Western Australia (Hammersley Group) was located basinward of a shelf-slope break, whereas the Southern African record (Chuniespoort-Ghaap Group) was mostly deposited shoreward of a similar break (cf. de Kock et al., 2009). This break equates roughly to the Poonda Fault in Australia and the Griquatown Fault zone in Southern Africa, both of which delimit the extents of orogenesis that post-dates the GOE and deformed the craton margins in both regions (Fig. 4). However, deposition of the diamictites was controlled by different sedimentary polarities, with the Makganyene Formation derived from the Ghaap platform shoreward of the slope break (Moore et al., 2012; Polteau et al., 2006), whereas all diamictites in the Turee Creek Group were derived from uplifted Hammersley Group rocks basinward of the break, in the hinterland of the Ophthalmia Orogeny (Martin, 1999, 2020). It is important to note that Clendenin (1989) documents a period of moderate folding prior to development of the mid-Duitschland unconformity, and Beukes and Gutzmer (2008) similarly document post-Mooiandraai folding that they correlate with the Ophthalmia Orogeny in Australia. These observations call into question interpretations of a rift setting for the Pretoria and Postmasburg Groups (e.g. Catuneanu and Eriksson, 2002; Eriksson et al., 2001), and strongly suggest a foreland basin setting like that of the correlative succession in Western Australia. In this interpretation, folding and unconformities developed east of the Griquatown Fault zone (Figs. 3 and 4;) possibly relate to a change in tectonic style (Martin et al., 1998) that could be interpreted in terms of forebulge uplift (cf. Martin, 2020).

4.2. North America

The North American stratigraphic record in the Lake Superior region, typified by the Huronian Supergroup and its correlatives such as the Snowy Pass Supergroup (e.g. Ojakangas et al., 2001b; Young, 2019), is globally important as the type area of Paleoproterozoic glacial diamictites (Fig. 3) that are closely associated with the GOE, but the climatic constraints from other proxies are poor in this region. In particular, the disappearance of S-MIF (Cui et al., 2018) is very poorly constrained due to local and regional unconformities and the absence of suitable lithologies in key parts of the record. Geochronological constraints are also poor, but the presence of four discrete glacial diamictite horizons, two of which are in the Gowganda Formation and are commonly considered the product of a single glaciation, could potentially allow a direct correlation with Western Australia. However, the reliability of such a direct lithological correlation awaits corroborating evidence from geochronology and other proxies of the GOE in both regions. The stratigraphic record in this region also suffers from similar outcrop continuity issues to Southern Africa, with the two oldest diamictite horizons only known from two localities (Young, 2019), which adds additional uncertainty to regional and global correlations. However, assuming current age constraints are more robust than the S-MIF record for correlation, all of the stratigraphically discrete diamictite horizons in the Huronian Supergroup are older than the Meteorite Bore Member (Fig. 3), which precludes direct correlation with the MBS. Furthermore, Kopp et al. (2005) interpreted that all three interpreted Huronian glaciation events predate the Makganyene glaciation in Southern Africa, implying that global correlation of these events as

represented by diamictites is not supported by available data.

4.3. Fennoscandia

The importance of the Fennoscandian stratigraphic record lies in an interpreted loss of S-MIF that predates that of Southern Africa (Warke et al., 2020) and in the presence of Paleoproterozoic glacial diamictites (e.g. Melezhik et al., 2005; Ojakangas et al., 2001a; Strand, 2012; Strand and Laajoki, 1993). Studies in Western Australia have also suggested the presence of ‘whiffs of oxygen’ before the GOE (Anbar et al., 2007), although the significance of this record has recently been called into question (Uveges et al., 2023; Slotznick et al., 2022). Confirmation of any loss of S-MIF prior to 2.3 Ga is critical to determining the timing and trajectory of the GOE, and the relatively conformable and unmetamorphosed stratigraphic record across this interval in the MBS is critical to the resolution of this issue. Global correlation of the Fennoscandian record is hampered by a lack of adequate geochronological constraints, but the apparent loss of S-MIF between the Seidorechka and Polisarka Sedimentary Formations (Warke et al., 2020) equates broadly to the upper part of the Hamersley Group, above the Brockman Iron Formation. Consequently, this interval should be targeted for more detailed MSI analysis.

5. Insights from the Mount Bruce Supergroup

The Western Australian record of the Archean-Proterozoic transition, as recorded in the MBS, and its correlation with other successions of similar age provides some important insights into the consequences of revising the APB based on the record of the GOE. The first is that if the revised boundary is to be based on current definitions of the GOE using the S-MIF record, then both the local and global S-isotope records are too biased and incomplete to be of practical use at this stage. However, with a relatively conformable stratigraphic record, spanning over 420 million years, the MBS should be the benchmark for all proxy records. Significant gaps in the MBS proxy records currently exist in key stratigraphic units in the Hamersley and Turee Creek Groups. Unfortunately, the outcrops are generally too weathered for most geochemical and isotopic proxy studies, and available drill cores do not intersect all relevant units. Completion of these records would therefore require additional targeted drilling.

Given the incomplete and biased nature of the MSI record (Uveges et al., 2023) upon which definition of the GOE, and by extension proposals for a revised APB, is based, physical proxies would provide a more practical definition. Two options have so far been advocated for a revised APB, namely the first appearance of glacial diamictites (Van Kranendonk et al., 2012) and the disappearance of Hamersley-style BIF (Shields et al., 2022). In Australia both these options correspond broadly with the contact between the Hamersley and Turee Creek Groups, and specifically with the lower and upper contacts respectively of the Cave Hill Member of the Boolgeeda Iron Formation (Fig. 3). The equivalent interval in Southern Africa is potentially between the base of the Doradale diamictite in the Koegas Subgroup, and the top of the Hotazel Formation in the Postmasburg Group. However, more work is required to determine the extent and significance of lesser known diamictite horizons in Southern Africa. The absence of BIF, limited outcrop of older diamictite and poor age constraints in the Huronian Supergroup, and other similar areas such as Fennoscandia, will make global correlation of a revised APB on this basis quite challenging. Nonetheless, the rapid decline in BIF deposition that is coincident with a rapid initiation of a prolonged period of glaciation and diamictite deposition would seem to be an appropriate basis for revision of the APB that would also more precisely define the ‘Archean-Proterozoic transition’. Furthermore, the evidence from facies associated with the diamictites in Australia and Southern Africa (mafic volcanic rocks, stromatolitic carbonates), combined with sparse paleomagnetic evidence (Evans et al., 1997), suggests that few of these glaciations were global in nature (cf. Bekker et al.,

2020), thereby downplaying the value of individual diamictite horizons for global correlation.

Chronostratigraphic revision of the APB and its associated GSSP also depends on precise age constraints. Although the geochronology of the lower part of the MBS is now well constrained, this is not the case for the key interval around uppermost Hamersley Group and lower Turee Creek Group. All the existing age constraints in this interval are based on maximum depositional ages from detrital zircon (see Martin, 2020 for a review) because there are no known primary volcaniclastic tuff beds suitable for dating. However, whole-rock Re–Os isochron dating has recently produced results that are stratigraphically consistent with U–Pb zircon maximum depositional ages (Philippot et al., 2018; Anbar et al., 2007) and holds significant potential for improving the geochronological constraints in future. The identification of unconformities and depositional hiatuses associated with the proposed revised APB, prevents the accurate application of depositional rates for age estimates, and also affects the interpretation of maximum depositional ages. Age constraints from the MBS and Transvaal Supergroup suggest that the revised APB should be between c. 2.44 and 2.42 Ga (Fig. 3), although there appears to be greater potential to improve the precision of these ages in Southern Africa and the boundary is probably closer to 2.42 Ga (Van Kranendonk et al., 2012; Martin and Howard, 2023).

An important consequence of a chronostratigraphic revision of the APB to c. 2.42 Ga is that the Siderian Period will become the last of the Archean Eon, and a new period will need to be defined at the start of the revised Paleoproterozoic Era (Fig. 2). This is therefore a good opportunity to redefine the Siderian, which currently does not include one of the most important of the Hamersley BIF horizons, the Marra Mamba Iron Formation. Here we propose that any revision of the Siderian should include all Superior/Hamersley-style platform BIFs (c.f. Bekker et al., 2010) > 2.42 Ga, which in the MBS would include the Marra Mamba Iron Formation that would constrain the maximum age of this period to 2629 Ma (Trendall et al., 2004). This definition would also include the peak of this style of BIF deposition, typified by the 360 m-thick Joffre Member of the Brockman Iron Formation, but would exclude the younger Superior-style iron formations of North America. Whilst this definition is primarily based on the stratigraphic record of the MBS, additional criteria need to be added to cover areas such as Southern Africa where the period would not be characterized by iron formation in its early stages (Fig. 3). This period might also include proxy records of an extended GOE, perhaps affecting primarily the oceanic realm prior to the rise of atmospheric O₂ (Kaufman et al., 2007). The regional and global differences of expression highlight the importance of spatially and temporally constrained GSSPs in chronostratigraphic definition.

The loss of extensive BIF from the global stratigraphic record, and the first appearance of glacial diamictite in Australia and Southern Africa at the termination of the Siderian likely reflects the consequences of rising oceanic and atmospheric O₂ concentrations that drove cooling via the oxidation of methane (Goldblatt et al., 2006; Kopp et al., 2005) and a reduced greenhouse effect. Revised global correlation (Fig. 3) suggests that the record of this transition is more complete and has better geochronological constraints in Southern Africa where it occurred at c. 2424 Ma and may have predated the same transition in Western Australia. Better geochronological constraints are required in both areas to determine where an associated GSSP should be placed. A further consequence of a revised APB at c. 2.42 Ga is that regardless of which of the two proposed boundary definitions are adopted, some Hamersley Group BIF will belong to the new Paleoproterozoic period, or some diamictite will belong in the Siderian (Fig. 3). Consequently, the choice of APB needs to be carefully considered before ratification.

We propose that the new period marking the start of the Paleoproterozoic Era be defined based on physical rather than geochemical proxies of the GOE. The most conspicuous proxy would be the presence of glacial diamictites, which global correlation based on currently available stratigraphic and geochronological data shows cannot be readily correlated (Fig. 3). Interpretations that involve global diamictite

correlation generally assume there were three to four Paleoproterozoic glacial events, but opinions differ as to how many can be considered the product of 'snowball Earth' conditions (e.g. Bekker et al., 2020; Young, 2019). The logical consequence of the current stratigraphic constraints is that glaciogenic diamictites were deposited over a timespan of about 190 my in the early Paleoproterozoic, and that these deposits could be used to define a new period. The Makganyene Formation in South Africa is the only diamictite-bearing unit with low-latitude paleomagnetic constraints (Evans et al., 1997), suggesting that this interval and its potential direct correlatives (Fig. 3) are the only likely record of a 'snowball Earth' event (Kirschvink et al., 2000). This interpretation is supported by the presence of unambiguous dropstones in the Cave Hill Member (Martin, 1999; Van Kranendonk et al., 2015b). Evidence for open- and shallow-water to emergent depositional conditions associated with all other diamictites in the MBS (Krapež et al., 2017; Krapež, 1996; Martin, 2020; Martin et al., 2000; Martin and Howard, 2023; Mazumder et al., 2015; Van Kranendonk et al., 2015a; Van Kranendonk et al., 2015b; Van Kranendonk and Mazumder, 2015) does not support a 'snowball Earth' scenario for the remainder of the Australian succession. Consequently, direct or indirect evidence of 'snowball Earth' conditions might also be used to define the base of a new period at the start of the Paleoproterozoic.

This new period typified by glaciogenic deposits would also be characterized by other physical proxies of an oxygenated atmosphere/ocean system, such as red beds, the first appearance of sulphate evaporites, and the first extensive sedimentary manganese deposits typified by those of the Kalahari manganese field in South Africa (Fig. 3). This definition would also include geochemical proxies of an oxidising atmosphere, including the current definition of the GOE as determined by the S-isotope record. On this basis, and following the conventions for other chronostratigraphic units, we suggest a name based on the Greek etymology for either ice (πάγος, πάγος) or glacial (παγετώδης, παγετώδης), as an alternative to 'Skourian' (Shields et al., 2022). If the base is placed at the first occurrence of diamictite in the MBS, it would equate to an age of c. 2429 Ma, based on a BIF depositional rate of 10 m/my for the underlying 150 m of Boolgeeda Iron Formation above the c. 2444 Ma Woongarra Rhyolite. However, this estimate applies the same depositional rate to non-BIF lithologies in that interval and does not account for the duration of the disconformity at the base of the Boolgeeda Iron Formation and is therefore open to revision.

6. Conclusions

The chronometric Archean–Proterozoic boundary (APB) as currently defined at 2500 Ma has served the geoscience community well for over three decades and is considered an acceptable interim measure until a more practical chronostratigraphic boundary can be defined and agreed upon. Retention of this boundary as a chronostratigraphic one based on chemostratigraphy (Gaucher and Frei, 2018) is therefore plausible. However, a consensus is emerging to revise the boundary to coincide with the initiation of the GOE, although a precise definition of what constitutes this event, and its timing, remains controversial. Nonetheless the GOE is arguably one of the most significant events in Earth history without which complex life as we know it would not have evolved and it is thus an appropriate basis for a revised APB. However, the GOE as currently defined based on the influence of atmospheric O₂ on the sulfur cycle (Farquhar et al., 2000), like the chronometric APB, cannot be accurately placed or geochronologically constrained in any stratigraphic section. Also, the uncertainties in the nature of the GOE and the need to conduct detailed isotopic studies to identify it, make the event itself a very impractical basis for a revised APB. Physical proxies that are either direct or indirect products of oxygenation of the atmosphere would be more easily identified and practically applied.

In this regard, the appearance of glacial diamictites associated with the GOE, interpreted to reflect cooling due to oxidation of methane by atmospheric O₂ (Goldblatt et al., 2006; Kopp et al., 2005), has been

proposed as the basis of a revised APB (Van Kranendonk et al., 2012). Alternatively, the end of major Archean BIF deposition has been suggested as a basis for revision (Shields et al., 2022). Both events are recorded in the MBS and are closely associated with the c. 2.4 Ga contact between the Hamersley and Turee Creek Groups. A revision based on either of these options would necessitate defining the Siderian as the terminal period of the Neoproterozoic Era, and a new period would be required at the base of the Paleoproterozoic Era. Names that have been suggested for this new period are based on a definition that emphasises the GOE (Fig. 3; Van Kranendonk et al., 2012; Shields et al., 2022), but a name that reflects the many glacial diamictite horizons that characterize the physical rock record of this interval is perhaps more appropriate (Martin and Howard, 2023). Irrespective of the final boundary selection, this new period would contain the GOE as originally defined by Farquhar et al. (2000). The main defining characteristic of the APB would then be the rapid decline in Neoproterozoic BIF deposition accompanied by the appearance of several physical and chemical proxies of an oxygenated atmosphere, most notably glacial diamictites and the loss of S-MIF, over a relatively short time span (cf. Gaucher and Frei, 2018).

The exact placement of this boundary needs to be carefully considered along with the definition of the adjoining periods. Stratigraphic records in both Western Australia and Southern Africa show that if the boundary is placed at the base of the first diamictite, some Siderian-style BIF will be placed in the revised Paleoproterozoic, and similarly if the end of BIF deposition is chosen, some diamictite will be Neoproterozoic. There is also the problem of unconformities associated with this transition in both areas. However, in the MBS the first appearance of diamictite and last of BIF are within about 10 m of each other, corresponding to the base and top of the Cave Hill Member of the Boolgeeda Iron Formation, respectively. This constrains an APB based on either of these definitions to c. 2420 Ma (Van Kranendonk et al., 2012; Martin, 2020). However, this age should be revised based on better age constraints and global correlations.

CRedit authorship contribution statement

David McB Martin: Conceptualization, Visualization, Writing – original draft, Writing – review & editing. **Indrani Mukherjee:** Writing – original draft, Writing – review & editing. **Alex J. McCoy-West:** Writing – original draft, Writing – review & editing. **Heather M. Howard:** Writing – original draft, Writing – review & editing.

Declaration of competing interest

The authors declare that they have no known competing financial interests or personal relationships that could have appeared to influence the work reported in this paper.

Data availability

No data was used for the research described in the article.

Acknowledgements

DM acknowledges the significant influence that the work of Bill Clendenin, Chris Powell and Nic Beukes have had on developing the correlations we present. Bill sadly passed away about a year before Nic, who it was hoped might make it to 6IAS, and we dedicate this paper to their memory and contributions to Vaalbara geology. Andrey Bekker declined to contribute to this paper, but we thank him for his thought-provoking Keynote that stimulated a lot of post-conference re-evaluation and refinement of the ideas presented in the fieldguide. We also thank Ben Uveges for discussions regarding the Sulfur isotope record and David Evans for clarifying constraints on the Paleoproterozoic 'snowball Earth' hypothesis. Two anonymous reviewers also alerted us to some important omissions and misunderstandings that have helped

improve the final manuscript. The authors would particularly like to thank all those who attended the 6IAS fieldtrip, and Michael Prause for drafting. AMW acknowledges ARC grant DE210101395. DM and HH publish with permission of the Director, Geological Survey of Western Australia.

References

- Albut, G., Babechuk, M.G., Kleinhans, I.C., Bengler, M., Beukes, N.J., Steinhilber, B., Smith, A.J., Kruger, S.J., Schoenberg, R., 2018. Modern rather than Mesoproterozoic oxidative weathering responsible for the heavy stable Cr isotopic signatures of the 2.95 Ga old Ijzermijn iron formation (South Africa). *Geochim. Cosmochim. Acta* 228, 157–189. <https://doi.org/10.1016/j.gca.2018.02.034>.
- Anbar, A.D., Buick, R., Gordon, G.W., Johnson, A.C., Kendall, B., Lyons, T.W., Ostrander, C.M., Planavsky, N.J., Reinhard, C.T., Stüeken, E.E., 2023. Technical comment on “Reexamination of 2.5-Ga ‘whiff’ of oxygen interval points to anoxic ocean before GOE”. *Sci. Adv.* 9, eabq3736. <https://doi.org/10.1126/sciadv.abq3736>.
- Anbar, A., Duan, Y., Lyons, T.W., Arnold, G.L., Kendall, B., Creaser, R.A., Kaufman, A.J., Gordon, G.W., Scott, C., Garvin, J., Buick, R., 2007. A whiff of oxygen before the great oxidation event? *Science* 317, 1903–1906.
- Árting, T.B., Boggiani, P.C., Gaucher, C., Fernandes, H.A., Frei, R., 2023. Strong positive fractionation of chromium isotopes in iron formation of the Jacadigo Group (Brazil) – a link to enhanced atmospheric oxygenation during the Late Neoproterozoic. *Gondw. Res.* 124, 39–60.
- Barley, M.E., Pickard, A.L., Sylvester, P.J., 1997. Emplacement of a large igneous province as a possible cause of banded iron-formation 2.45 billion years ago. *Nature* 385, 55–58.
- Battistuzzi, F.U., Feijao, A., Hedges, S.B., 2004. A genomic timescale of prokaryote evolution: insights into the origin of methanogenesis, phototrophy, and the colonization of land. *BMC Evol. Biol.* 4, 44. <https://doi.org/10.1186/1471-2148-4-44>.
- Bédard, J.H., 2018. Stagnant lids and mantle overturns: implications for Archean tectonics, magmagenesis, crustal growth, mantle evolution, and the start of plate tectonics. *Geosci. Front.* 9, 19–49. <https://doi.org/10.1016/j.gsf.2017.01.005>.
- Bekker, A., Kaufman, A.J., Karhu, J.A., Beukes, N.J., Swart, Q., Coetzee, L.L., Eriksson, K.A., 2001. Chemostratigraphy of the Paleoproterozoic Deutschland Formation, South Africa — Implications for coupled climate change and carbon cycling. *Am. J. Sci.* 301, 261–285.
- Bekker, A., Holland, H.D., Wang, P.-L., Rumble III, D., Stein, H.J., Hannah, J.L., Coetzee, L.L., Beukes, N.J., 2004. Dating the rise of atmospheric oxygen. *Nature* 427, 117–120.
- Bekker, A., Karhu, J.A., Kaufman, A.J., 2006. Carbon isotope record for the onset of the Lomagundi carbon isotope excursion in the Great Lakes area, North America. *Precamb. Res.* 148, 145–180. <https://doi.org/10.1016/j.precamres.2006.03.008>.
- Bekker, A., Slack, J.F., Planavsky, N.J., Krapež, B., Hofmann, A.W., Konhauser, K.O., Rouxel, O.J., 2010. Iron formation: the sedimentary product of a complex interplay among mantle, tectonic, oceanic, and biospheric processes. *Econ. Geol.* 105, 467–508.
- Bekker, A., Krapež, B., Karhu, J.A., 2020. Correlation of the stratigraphic cover of the Pilbara and Kaapvaal cratons recording the lead up to Paleoproterozoic Icehouse and the GOE. *Earth Sci. Rev.* 211, 1–32. <https://doi.org/10.1016/j.earscirev.2020.103389>.
- Beukes, N.J., Gutzmer, J., 2008. Origin and paleoenvironmental significance of major iron formations at the Archean-Paleoproterozoic boundary. *Rev. Econ. Geol.* 15, 5–47. <https://doi.org/10.5382/Rev.15.01>.
- Blake, T.S., 2001. Cyclic continental mafic tuff and flood basalt volcanism in the Late Archean Nullagine and Mount Jope Supersequences in the eastern Pilbara, Western Australia. *Precamb. Res.* 107, 139–177.
- Blake, T.S., Barley, M.E., 1992. Tectonic evolution of the Late Archean to Early Proterozoic Mount Bruce megasequence set, Western Australia. *Tectonics* 11, 1415–1425.
- Blake, T.S., Groves, D.I., 1987. Continental rifting and the Archean-Proterozoic transition. *Geology* 15, 229–232.
- Bleeker, W., 2004. Towards a ‘natural’ timescale for the Precambrian – A proposal. *Lethaia* 37, 219–222.
- Brüske, A., Martin, A.N., Rammensee, P., Eroglu, S., Lazarov, M., Albut, G., Schuth, S., Aulbach, S., Schoenberg, R., Beukes, N., Hofmann, A., Nägler, T., Weyer, S., 2020. The onset of oxidative weathering traced by uranium isotopes. *Precamb. Res.* 338, 105583. <https://doi.org/10.1016/j.precamres.2019.105583>.
- Canfield, D.E., Ngombi-Pemba, L., Hammarlund, E.U., Bengtson, S., Chaussidon, M., Gauthier-Lafaye, F., Meunier, A., Riboulleau, A., Rollion-Bard, C., Rouxel, O., Asael, D., Pierson-Wickmann, A.-C., El Albani, A., 2013. Oxygen dynamics in the aftermath of the Great Oxidation of Earth’s atmosphere. *PNAS* 110, 16736–16741. <https://doi.org/10.1073/pnas.1315570110>.
- Caquingneau, T., Paquette, J.-L., Philippot, P., 2018. U-Pb detrital zircon geochronology of the Turee Creek Group, Hamersley Basin, Western Australia: timing and correlation of the Paleoproterozoic glaciations. *Precamb. Res.* 307, 34–50.
- Catuneanu, O., Eriksson, P.G., 2002. Sequence stratigraphy of the Precambrian Rooihogte–Timeball Hill rift succession, Transvaal Basin, South Africa. *Sed. Geol.* 147, 71–88.
- Cawood, P.A., Hawkesworth, C.J., Dhuime, B., 2013. The continental record and the generation of continental crust. *J. Geol. Soc. London* 125, 14–32. <https://doi.org/10.1130/B30722.1>.
- Cawood, P.A., Hawkesworth, C.J., Pisarevsky, S.A., Dhuime, B., Capitanio, F.A., Nebel, O., 2018. Geological archive of the onset of plate tectonics. *Philos. Trans. R. Soc. A Math. Phys. Eng. Sci.* 376, 0170405. <https://doi.org/10.1098/rsta.2017.0405>.
- Cheney, E.S., 1996. Sequence stratigraphy and plate tectonic significance of the Transvaal succession of southern Africa and its equivalent in Western Australia. *Precamb. Res.* 79, 3–24.
- Cheney, E.S., Roering, C., Winter, H. de la R., 1990. The Archean-Proterozoic boundary in the Kaapvaal Province of Southern Africa. *Precamb. Res.* 46, 329–340.
- Clendenin, C.W., 1989. Tectonic influence on the evolution of the Early Proterozoic Transvaal Sea, Southern Africa. PhD. Johannesburg, p. 367.
- Clendenin, C.W., Charlesworth, E.G., Maske, S., 1988. An early Proterozoic three-stage rift system, Kaapvaal Craton, South Africa. *Tectonophysics* 145, 73–86. [https://doi.org/10.1016/0040-1951\(88\)90317-4](https://doi.org/10.1016/0040-1951(88)90317-4).
- Cloud, P., 1972. A working model of the primitive earth. *Am. J. Sci.* 272, 537–548.
- Cloud, P., 1987. Trends, transitions, and events in cryptozoic history and their calibration: apropos recommendations by the Subcommission on Precambrian Stratigraphy. *Precamb. Res.* 37, 257–264.
- Cloud, P., 1976. Major features of crustal evolution. Geological Society of South Africa. Alex L. Du Toit Memorial Lecture Series, 1976.
- Coetzee, I.I., 2001. Genetic stratigraphy of the Paleoproterozoic Pretoria Group in the western Transvaal. MSc, Johannesburg, p. 212.
- Cohen, K.M., Finney, S.C., Gibbard, P.L., Fan, J.-X., 2013. The ICS International Chronostratigraphic Chart. *Episodes* 36, 199–204.
- Condie, K.C., Des Marais, D.J., Abbott, D., 2001. Precambrian superplumes and supercontinents: a record in black shales, carbon isotopes, and paleoclimates? *Precamb. Res.* 106, 239–260. [https://doi.org/10.1016/S0301-9268\(00\)00097-8](https://doi.org/10.1016/S0301-9268(00)00097-8).
- Condie, K.C., O’Neill, C., 2010. The Archean-Proterozoic boundary: 500 My of tectonic transition in earth history. *Am. J. Sci.* 310, 775–790. <https://doi.org/10.2475/09.2010.01>.
- Crook, K.A.W., 1989. Why the precambrian time-scale should be chronostratigraphic: a response to recommendations by the Subcommission on Precambrian stratigraphy. *Precamb. Res.* 43, 143–150.
- Cui, H., Kitajima, K., Spicuzza, M.J., Fournelle, J.H., Ishida, A., Brown, P.E., Valley, J.W., 2018. Searching for the Great Oxidation Event in North America: a reappraisal of the Huronian Supergroup by SIMS sulfur four-isotope analysis. *Astrobiology* 18, 519–538. <https://doi.org/10.1089/ast.2017.1722>.
- de Kock, M.O., Evans, D.A.D., Beukes, N.J., 2009. Validating the existence of Vaalbara in the Neoproterozoic. *Precamb. Res.* 174, 145–154.
- Dorland, H.C., 1999. Paleoproterozoic laterites, red beds and ironstones of the Pretoria group with reference to the history of atmospheric oxygen. MSc, Johannesburg, p. 147.
- Dunn, P.R., Plumb, K.A., Roberts, H.G., 1966. A proposal for time-stratigraphic subdivision of the Australian Precambrian. *J. Geol. Soc. Aust.* 13, 593–608. <https://doi.org/10.1080/00167616608728634>.
- Eriksson, P.G., Altermann, W., Catuneanu, O., van der Merwe, R., Bumby, A.J., 2001. Major influences on the evolution of the 2.67–2.1 Ga Transvaal basin, Kaapvaal Craton. *Sedimentary Geology* 141–142, 205–231. [https://doi.org/10.1016/S0037-0738\(01\)00075-6](https://doi.org/10.1016/S0037-0738(01)00075-6).
- Evans, D.A.D., Beukes, N.J., Kirschvink, J.L., 1997. Low-latitude glaciation in the Paleoproterozoic era. *Nature* 386, 262–266.
- Fakhraee, M., Tarhan, L.G., Reinhard, C.T., Crowe, S.A., Lyons, T.W., Planavsky, N.J., 2023. Earth’s surface oxygenation and the rise of eukaryotic life: relationships to the Lomagundi positive carbon isotope excursion revisited. *Earth Sci. Rev.* 240, 104398. <https://doi.org/10.1016/j.earscirev.2023.104398>.
- Farquhar, J., Bao, H., Thieme, M., 2000. Atmospheric influence of Earth’s earliest sulfur cycle. *Science* 289, 756–758. <https://doi.org/10.1126/science.289.5480.756>.
- Farquhar, J., Zerkle, A.L., Bekker, A., 2011. Geological constraints on the origin of oxygenic photosynthesis. *Photosynth. Res.* 107, 11–36. <https://doi.org/10.1007/s11220-010-9594-0>.
- Frei, R., Gaucher, C., Poulton, S.W., Canfield, D.E., 2009. Fluctuations in Precambrian atmospheric oxygenation recorded by chromium isotopes. *Nature* 461, 250–253. <https://doi.org/10.1038/nature08266>.
- Gardiner, N.J., Hickman, A.H., Kirkland, C.L., Lu, Y., Johnson, T., Zhao, J.-X., 2017. Processes of crust formation in the early Earth imaged through Hf isotopes from the East Pilbara Terrane. *Precamb. Res.* 297, 56–76. <https://doi.org/10.1016/j.precamres.2017.05.004>.
- Gaucher, C., Frei, R., 2018. The archean-proterozoic boundary and the great oxidation event. In: Sial, A.N., Gaucher, C., Ramkumar, M., Ferreira, V.P. (Eds.), *Chemostratigraphy Across Major Chronological Boundaries*. John Wiley & Sons Inc, pp. 35–45.
- Goldblatt, C., Lenton, T.M., Watson, A.J., 2006. Bistability of atmospheric oxygen and the Great Oxidation. *Nature* 443, 683–686. <https://doi.org/10.1038/nature05169>.
- Golden, J.J., 2019. Mineral Evolution Database: Data Model for Mineral Age Associations. MSc. Tucson, Arizona.
- Gregory, D.D., Large, R.R., Halpin, J.A., Steadman, J.A., Hickman, A.H., Ireland, T.R., Holden, P., 2015. The chemical conditions of the late Archean Hamersley basin inferred from whole rock and pyrite geochemistry with $\Delta 33S$ and $\delta 34S$ isotope analyses. *Geochim. Cosmochim. Acta* 149, 223–250. <https://doi.org/10.1016/j.gca.2014.10.023>.
- Gregory, D., Mukherjee, I., Olson, S.L., Large, R.R., Danyushevsky, L.V., Stepanov, A.S., Avila, J.N., Cliff, J., Ireland, T.R., Raiswell, R., Olin, P.H., Maslennikov, V.V., Lyons, T.W., 2019. The formation mechanisms of sedimentary pyrite nodules determined by trace element and sulfur isotope microanalysis. *Geochim. Cosmochim. Acta* 259, 53–68. <https://doi.org/10.1016/j.gca.2019.05.035>.

- Gumsley, A.P., Chamberlain, K.R., Bleeker, W., Söderlund, U., de Kock, M.O., Larsson, E. R., Bekker, A., 2017. Timing and tempo of the Great Oxidation Event. *PNAS* 114, 1811–1816. <https://doi.org/10.1073/pnas.1608824114>.
- Halligan, R., Daniels, J.L., 1964. Precambrian geology of the Ashburton Valley Region, north-west division, in: Annual report for the year 1963. Geological Survey of Western Australia, pp. 38–46.
- Havsteen, J.C., Kleinhans, I.C., Schröder, S., Eickmann, B., Izon, G., Gogouvtis, M.D., Ngobeli, R., Beukes, N.J., Schoenberg, R., 2023. Evidence for contemporaneous deposition of the Duitschland and Rooihooft formations (Transvaal supergroup): implications for tempo and mode of Earth's Great Oxidation. *Precamb. Res.* 391, 107055 <https://doi.org/10.1016/j.precambres.2023.107055>.
- Hickman, A.H., 2004. Two contrasting granite–greenstones terranes in the Pilbara Craton, Australia: evidence for vertical and horizontal tectonic regimes prior to 2900 Ma. *Precamb. Res.* 131, 153–172.
- Hickman, A.H., Van Kranendonk, M.J., 2012. Early earth evolution: evidence from the 3.5 – 1.8 Ga geological history of the Pilbara region of Western Australia. *Episodes* 35, 283–297. <https://doi.org/10.18814/epiuiugs/2012/v35i1/028>.
- Hofmann, H.J., 1990. Precambrian time units and nomenclature – the geon concept. *Geology* 18, 340–341.
- Holland, H.D., 1999. When did the Earth's atmosphere become Oxidic? A Reply. *Newsletter of the Geochemical Society* 100, 20–22.
- Holland, H.D., 2002. Volcanic gases, black smokers and the Great Oxidation Event. *Geochim. Cosmochim. Acta* 66, 3811–3826.
- Holland, H.D., 2006. The oxygenation of the atmosphere and oceans. Philosophical transactions of the Royal Society of London. Series b, Biological Sciences 361, 903–915. <https://doi.org/10.1098/rstb.2006.1838>.
- Humbert, F., de Kock, M.O., Altermann, W., Elburg, M.A., Lenhardt, N., Smith, A.J.B., Masango, S., 2018. Petrology, physical volcanology and geochemistry of a Paleoproterozoic large igneous province: the Hekpoort Formation in the southern Transvaal sub-basin (Kaaopvaal craton). *Precamb. Res.* 315, 232–256. <https://doi.org/10.1016/j.precambres.2018.07.022>.
- Izon, G., Luo, G., Uveges, B.T., Beukes, N., Kitajima, K., Ono, S., Valley, J.W., Ma, X., Summons, R.E., 2022. Bulk and grain-scale minor sulfur isotope data reveal complexities in the dynamics of Earth's oxygenation. *PNAS* 119. <https://doi.org/10.1073/pnas.2025606119> e2025606119.
- James, H.L., 1978. Subdivision of the Precambrian — A brief review and a report on recent decisions by the subcommission on Precambrian Stratigraphy. *Precamb. Res.* 7, 193–204. [https://doi.org/10.1016/0301-9268\(78\)90038-4](https://doi.org/10.1016/0301-9268(78)90038-4).
- Johnson, T.E., Brown, M., Gardiner, N.J., Kirkland, C.L., Smithies, R.H., 2017. Earth's first stable continents did not form by subduction. *Nature* 543, 239–242.
- Johnson, J.E., Webb, S.M., Thomas, K., Ono, S., Kirschvink, J.L., Fischer, W.W., 2013. Manganese-oxidizing photosynthesis before the rise of cyanobacteria. *PNAS* 110, 11238–11243. <https://doi.org/10.1073/pnas.1305530110>.
- Kaufman, A.J., Johnson, D.T., Farquhar, J., Masterson, A.L., Lyons, T.W., Bates, S., Anbar, A.D., Arnold, G.L., Garvin, J., Buick, R., 2007. Late Archean biospheric oxygenation and atmospheric evolution. *Science* 317, 1900–1903.
- Kendall, B., 2021. Recent advances in geochemical paleo-oxybarometers. *Annu. Rev. Earth Planet. Sci.* 49, 399–433. <https://doi.org/10.1146/annurev-earth-071520-051637>.
- Kendall, B., Creaser, R.A., Reinhard, C.T., Lyons, T.W., Anbar, A.D., 2015. Transient episodes of mild environmental oxygenation and oxidative continental weathering during the late Archean. *Sci. Adv.* 1, e1500777.
- Kepert, D.A., 2018. The mapped stratigraphy and structure of the mining area C region. Hamersley province, Geological Survey of Western Australia, p. 282.
- Killingsworth, B.A., Sansjofre, P., Philippot, P., Cartigny, P., Thomazo, C., Lalonde, S.V., 2019. Constraining the rise of oxygen with oxygen isotopes. *Nat Commun* 10, 4924. <https://doi.org/10.1038/s41467-019-12883-2>.
- Kirschvink, J.L., Gaidoes, E.J., Bertani, L.E., Beukes, N.J., Gutzmer, J., Maepa, L.N., Steinberger, R.E., 2000. Paleoproterozoic snowball Earth: extreme climatic and geochemical global change and its biological consequences. *PNAS* 97, 1400–1405.
- Knoll, A.H., Walter, M., Narbonne, G.M., Christie-Blick, N., 2004. A new period for the geological time scale. *Science* 305, 621–622.
- Koehler, M.C., Buick, R., Kipp, M.A., Stüeken, E.E., Zaloumis, J., 2018. Transient surface ocean oxygenation recorded in the ~2.66-Ga Jeerinah Formation. *Australia. PNAS* 115, 7711–7716. <https://doi.org/10.1073/pnas.1720820115>.
- Kopp, R.E., Kirschvink, J.L., Hilburn, I.A., Nash, C.Z., 2005. The Paleoproterozoic snowball Earth: a climate disaster triggered by the evolution of oxygenic photosynthesis. *PNAS* 102, 11131–11136. <https://doi.org/10.1073/pnas.0504878102>.
- Krapež, B., 1996. Sequence stratigraphic concepts applied to the identification of basin-filling rhythms in Precambrian successions. *Aust. J. Earth Sci.* 43, 355–380.
- Krapež, B., Müller, S.G., Fletcher, I.R., Rasmussen, B., 2017. A tale of two basins? Stratigraphy and detrital zircon provenance of the Paleoproterozoic Turee Creek and Horseshoe Basins of Western Australia. *Precamb. Res.* 294, 67–90.
- Kurzweil, F., Wille, M., Schoenberg, R., Taubald, H., Van Kranendonk, M.J., 2015. Continuously increasing $\delta^{98}\text{Mo}$ values in Neoproterozoic black shales and iron formations from the Hamersley Basin. *Geochim. Cosmochim. Acta* 164, 523–542.
- Lantink, M.L., Oonk, P.B.H., Floor, G.H., Tsikos, H., Mason, P.R., 2018. Fe isotopes of a 2.4 Ga hematite-rich IF constrain marine redox conditions around the GOE. *Precamb. Res.* 305, 218–235. <https://doi.org/10.1016/j.precambres.2017.12.025>.
- Lantink, M.L., Davies, J.H.F.L., Ovtcharova, M., Hilgen, F.J., 2022. Milankovitch cycles in banded iron formations constrain the Earth-Moon system 2.46 billion years ago. *PNAS* 119. <https://doi.org/10.1073/pnas.2117146119> e2117146119.
- Lantink, M.L., Lenstra, W.K., Davies, J.H.F.L., Hennekam, R., Martin, D.M., Mason, P.R., Reichart, G.-J., Slomp, C.P., Hilgen, F.J., 2023. Precessional pacing of early Proterozoic redox cycles. *Earth Planet. Sci. Lett.* 610, 118117 <https://doi.org/10.1016/j.epsl.2023.118117>.
- Large, R.R., Hazen, R.M., Morrison, S.M., Gregory, D.D., Steadman, J.A., Mukherjee, I., 2022. Evidence that the GOE was a prolonged event with a peak around 1900 Ma. *Geosystems and Geoenvironment* 1, 100036. <https://doi.org/10.1016/j.geogeo.2022.100036>.
- Lepot, K., 2020. Signatures of early microbial life from the Archean (4 to 2.5 Ga) eon. *Earth Sci. Rev.* 209, 103296 <https://doi.org/10.1016/j.earscirev.2020.103296>.
- Lindsay, J.F., Brasier, M.D., 2002. Did global tectonics drive early biosphere evolution? Carbon isotope record from 2.6 to 1.9 Ga carbonates of Western Australia. *Precamb. Res.* 114, 1–34.
- Luo, G., Ono, S., Beukes, N.J., Wang, D.T., Xie, S., Summons, R.E., 2016. Rapid oxygenation of Earth's atmosphere 2.33 billion years ago. *science*. *Advances* 2, e1600134.
- Lyons, T.W., Reinhard, C.T., Planavsky, N.J., 2014. The rise of oxygen in Earth's early ocean and atmosphere. *Nature* 506, 307–315.
- Lyons, T.W., Diamond, C.W., Planavsky, N.J., Reinhard, C.T., Li, C., 2021. Oxygenation, life, and the planetary system during Earth's middle history: an overview. *Astrobiology* 21, 906–923. <https://doi.org/10.1089/ast.2020.2418>.
- Martin, D.McB., 1990. Early proterozoic syndepositional tectonics along the Thabazimbi-Murchison line, west of Thabazimbi. *MSc. Johannesburg*, p. 214.
- Martin, D.McB., 1999. Depositional setting and implications of Paleoproterozoic glaciomarine sedimentation in the Hamersley Province, Western Australia. *Geol. Soc. Am. Bull.* 111, 189–203.
- Martin, D.McB., 2020. Geology of the Hardey Syncline — the key to understanding the northern margin of the Capricorn Orogen. *Geological Survey of Western Australia* 62, pp.
- Martin, D.McB., Clendenin, C.W., Krapež, B., McNaughton, N.J., 1998. Tectonic and geochronological constraints on late Archean and Palaeoproterozoic stratigraphic correlation within and between the Kaapvaal and Pilbara Cratons. *J. Geol. Soc. London* 155, 311–322.
- Martin, A.P., Condon, D.J., Prave, A.R., Lepland, A., 2013. A review of temporal constraints for the Palaeoproterozoic large, positive carbonate carbon isotope excursion (the Lomagundi-Jatuli Event). *Earth Sci. Rev.* 127, 242–261. <https://doi.org/10.1016/j.earscirev.2013.10.006>.
- Martin, D.McB., Howard, H.M., 2023. 6IAS: out with the old, in with the new - a traverse across the Archean-Proterozoic boundary in the Mount Bruce Supergroup. *Geological Survey of Western Australia, Perth, Western Australia*, p. 58.
- Martin, D.McB., Morris, P.A., 2010. Tectonic setting and regional implications of ca. 2.2 Ga mafic magmatism in the southern Hamersley Province, Western Australia. *Aust. J. Earth Sci.* 57, 911–931.
- Martin, D.McB., Powell, C.McA., George, A.D., 2000. Stratigraphic architecture and evolution of the early Paleoproterozoic McGrath trough, Western Australia. *Precamb. Res.* 99, 33–64.
- Martindale, C.M., Strauss, J.V., Sperling, E.A., Johnson, J.E., Van Kranendonk, M.J., Flannery, D., French, K., Lepot, K., Mazumder, R., Rice, M.S., Schrag, D.P., Summons, R., Walter, M., Abelson, J., Knoll, A.H., 2015. Sedimentology, chemostratigraphy, and stromatolites of lower Paleoproterozoic carbonates, Turee Creek group, Western Australia. *Precamb. Res.* 266, 194–211.
- Martini, J.E.J., 1979. A copper-bearing bed in the Pretoria Group in northeastern Transvaal. *Geokongress 77* vol. 6, 65–72.
- Mazumder, R., 2017. A tale of two basins?: stratigraphy and detrital zircon provenance of the Paleoproterozoic Turee Creek and Horseshoe basins of Western Australia: Discussion. *Precamb. Res.* 298, 462–471. <https://doi.org/10.1016/j.precambres.2017.06.026>.
- Mazumder, R., Van Kranendonk, M.J., Altermann, W., 2015. A marine to fluvial transition in the Paleoproterozoic koolbye Formation, Turee Creek Group, Western Australia. *Precamb. Res.* 258, 161–170.
- Mazumder, R., De, S., Sunder Raju, P.V., 2019. Archean-Paleoproterozoic transition: the Indian perspective. *Earth Sci. Rev.* 188, 427–440. <https://doi.org/10.1016/j.earscirev.2018.11.013>.
- McCoy-West, A.J., Chowdhury, P., Burton, K.W., Sossi, P., Nowell, G.M., Fitton, J.G., Kerr, A.C., Cawood, P.A., Williams, H.M., 2019. Extensive crustal extraction in Earth's early history inferred from molybdenum isotopes. *Nature Geosci* 12, 946–951. <https://doi.org/10.1038/s41561-019-0451-2>.
- Melezhik, V.A., Fallick, A.E., Hanski, E.J., Kump, L.R., Lepland, A., Prave, A.R., Strauss, H., 2005. Emergence of the aerobic biosphere during the Archean-Proterozoic transition: challenges of future research. *GSA Today* 15, 4–11.
- Molén, M.O., 2024. Geochemical proxies: Paleoclimate or paleoenvironment? *Geosystems and Geoenvironment* 3, 100238. <https://doi.org/10.1016/j.geogeo.2023.100238>.
- Moore, J.M., Polteau, S., Armstrong, R.A., Corfu, F., Tsikos, H., 2012. The age and correlation of the Postmasburg Group, southern Africa: constraints from detrital zircon grains. *J. Afr. Earth Sci.* 64, 9–19. <https://doi.org/10.1016/j.jafrearsci.2011.11.001>.
- Nelson, D.R., Trendall, A.F., Altermann, W., 1999. Chronological correlations between the Pilbara and Kaapvaal cratons. *Precamb. Res.* 97, 165–189.
- Ngobeli, R., 2019. A comparison between detrital zircon age populations of the Koegas Subgroup of the Ghaap Group and overlying Makganyene Diamictite of the Postmasburg Group, Transvaal Supergroup, Griqualand West Area. *MSc. Johannesburg*, p. 342.
- Ohmoto, H., Watanabe, Y., Ikemi, H., Poulson, R., Taylor, B.E., 2006. Sulphur isotope evidence for anoxic Archean atmosphere. *Nature* 442, 873–876.
- Ojakangas, R.W., Marmo, J.S., Heiskanen, K.I., 2001a. Basin evolution of the Paleoproterozoic Karelian Supergroup of the Fennoscandian (Baltic) Shield. *Sed. Geol.* 141–142, 255–285. [https://doi.org/10.1016/S0037-0738\(01\)00079-3](https://doi.org/10.1016/S0037-0738(01)00079-3).

- Ojakangas, R.W., Morey, G.B., Southwick, D.L., 2001b. Paleoproterozoic basin development and sedimentation in the Lake Superior region, North America. *Sed. Geol.* 141–142, 319–341.
- Ostrander, C.M., Johnson, A.C., Anbar, A.D., 2021. Earth's first redox revolution. *Annu. Rev. Earth Planet. Sci.* 49, 337–366. <https://doi.org/10.1146/annurev-earth-072020-055249>.
- Paiste, K., Lepland, A., Zerkle, A.L., Kirsimäe, K., Kreitsmann, T., Mänd, K., Romashkin, A.E., Rychanchik, D.V., Prave, A.R., 2020. Identifying global vs. basinal controls on Paleoproterozoic organic carbon and sulfur isotope records. *Earth Sci. Rev.* 207, 103230 <https://doi.org/10.1016/j.earscirev.2020.103230>.
- Pasquier, V., Bryant, R.N., Fike, D.A., Halevy, I., 2021. Strong local, not global, controls on marine pyrite sulfur isotopes. *Sci. Adv.* 7 <https://doi.org/10.1126/sciadv.abb7403>.
- Pavlov, A.A., Kasting, J.F., 2002. Mass-independent fractionation of sulfur isotopes in Archean sediments: strong evidence for an anoxic Archean atmosphere. *Astrobiology* 2, 27–41. <https://doi.org/10.1089/153110702753621321>.
- Payne, J.L., Boyer, A.G., Brown, J.H., Finnegan, S., Kowalewski, M., Krause, R.A., Lyons, S.K., McClain, C.R., McShea, D.W., Novack-Gottshall, P.M., Smith, F.A., Stempin, J.A., Wang, S.C., 2009. Two-phase increase in the maximum size of life over 3.5 billion years reflects biological innovation and environmental opportunity. *PNAS* 106, 24–27. <https://doi.org/10.1073/pnas.0806314106>.
- Pehrsson, S.J., Buchan, K.L., Eglinton, B.M., Berman, R.M., Rainbird, R.H., 2014. Did plate tectonics shutdown in the Palaeoproterozoic? a view from the Siderian geologic record. *Gondw. Res.* 26, 803–815. <https://doi.org/10.1016/j.gr.2014.06.001>.
- Philippot, P., Ávila, J.N., Killingsworth, B.A., Tessalina, S., Baton, F., Caquineau, T., Muller, E., Pecoito, E., Cartigny, P., Lalonde, S.V., Ireland, T.R., Thomazo, C., Van Kranendonk, M.J., Busigny, V., 2018. Globally asynchronous sulphur isotope signals require re-definition of the Great Oxidation Event. *Nat. Commun.* 9, 1–10. <https://doi.org/10.1038/s41467-018-04621-x>.
- Philippot, P., Killingsworth, B.A., Paquette, J.-L., Tessalina, S., Cartigny, P., Lalonde, S.V., Thomazo, C., Ávila, J.N., Busigny, V., 2021. Comment on “Correlation of the stratigraphic cover of the Pilbara and Kaapvaal cratons recording the lead up to Paleoproterozoic Icehouse and the GOE” by Andrey Bekker, Bryan Krapez, and Juha A. Karhu, 2020, *Earth Science Reviews*, doi: 10.1016/j.earscirev.2020.103389. *Earth-Science Reviews* 218, 103594. doi: 10.1016/j.earscirev.2021.103594.
- Planavsky, N.J., Asael, D., Hofmann, A., Reinhard, C.T., Lalonde, S.V., Knudsen, A., Wang, X., Ossa Ossa, F., Pecoito, E., Smith, A.J.B., Beukes, N.J., Bekker, A., Johnson, T.M., Konhauser, K.O., Lyons, T.W., Rouxel, O.J., 2014. Evidence for oxygenic photosynthesis half a billion years before the Great Oxidation Event. *Nat. Geosci.* 7, 283–286. <https://doi.org/10.1038/ngeo2122>.
- Plumb, K.A., 1991. New Precambrian time scale. *Episodes* 14, 139–140. <https://doi.org/10.18814/epiiugs/1991/v14i2/005>.
- Plumb, K.A., James, H.L., 1986. Subdivision of Precambrian time: Recommendations and suggestions by the subcommittee on Precambrian stratigraphy. *Precamb. Res.* 32, 65–92.
- Polteau, S., 2005. Early Proterozoic Makganyene glacial event in South Africa: its implication in sequence stratigraphy interpretation, paleoenvironmental conditions, and iron and manganese ore deposition. PhD. Grahamstown, South Africa, p. 215.
- Polteau, S., Moore, J.M., Tsikos, H., 2006. The geology and geochemistry of the Paleoproterozoic Makganyene diamictite. *Precamb. Res.* 148, 257–274. <https://doi.org/10.1016/j.precamres.2006.05.003>.
- Poultou, S.W., Bekker, A., Cumming, V.M., Zerkle, A.L., Canfield, D.E., Johnston, D.T., 2021. A 200-million-year delay in permanent atmospheric oxygenation. *Nature* 592, 232–236. <https://doi.org/10.1038/s41586-021-03393-7>.
- Prave, A.R., Kirsimäe, K., Lepland, A., Fallick, A.E., Kreitsmann, T., Deines, Y., Romashkin, A.E., Rychanchik, D.V., Medvedev, P.V., Moussavou, M., Bakakas, K., Hodgskiss, M., 2022. The grandest of them all: the Lomagundi–Jatuli Event and Earth's oxygenation. *Jgs2021-036 JGS* 179. <https://doi.org/10.1144/jgs2021-036>.
- Rasmussen, B., Blake, T.S., Fletcher, I.R., 2005a. U–Pb zircon age constraints on the Hamersley spherule beds: evidence for a single 2.63 Ga Jeerinah–Carawue impact ejecta layer. *Geology* 33, 725–728.
- Rasmussen, B., Fletcher, I.R., Sheppard, S., 2005b. Isotopic dating of the migration of a low-grade metamorphic front during orogenesis. *Geology* 33, 773–776.
- Rasmussen, B., Bekker, A., Fletcher, I.R., 2013. Correlation of Paleoproterozoic glaciations based on U–Pb zircon ages for tuff beds in the Transvaal and Huronian Supergroups. *Earth Planet. Sci. Lett.* 382, 173–180.
- Reinhard, C.T., Planavsky, N.J., Lyons, T.W., 2013. Long-term sedimentary recycling of rare sulphur isotope anomalies. *Nature* 497, 100–103. <https://doi.org/10.1038/nature12021>.
- Robb, L.J., Knoll, A.H., Plumb, K.A., Shields, G.A., Strauss, H., Veizer, J., 2004. The Archean and Proterozoic Eons. In: Gradstein, F.M., Ogg, J.G., Smith, A.G. (Eds.), *A Geologic Time Scale*. Cambridge University Press, Cambridge, UK, pp. 129–140.
- Robbins, L.J., Fakhrae, M., Smith, A.J., Bishop, B.A., Swanner, E.D., Peacock, C.L., Wang, C.-L., Planavsky, N.J., Reinhard, C.T., Crowe, S.A., Lyons, T.W., 2023. Manganese oxides, Earth surface oxygenation, and the rise of oxygenic photosynthesis. *Earth Sci. Rev.* 239, 104368 <https://doi.org/10.1016/j.earscirev.2023.104368>.
- Rodrigues, P.de O.C., Hinnov, L.A., Franco, D.R., 2019. A new appraisal of depositional cyclicity in the Neoproterozoic Paleoproterozoic Dales Gorge Member (Brockman Iron Formation, Hamersley Basin, Australia). *Precamb. Res.* 328, 27–47.
- Roscoe, S.M., 1973. The Huronian Supergroup, a Paleoproterozoic succession showing evidence of atmospheric evolution. *Geol. Assoc. Can. Spec. Pap.* 12, 31–47.
- Roscoe, S.M., 1969. Huronian Rocks and Uraniferous Conglomerates in the Canadian Shield. Paper 68–40. Geological Survey of Canada, Ottawa, Canada.
- Rye, R., Holland, H.D., 1998. Paleosols and the evolution of atmospheric oxygen: a critical review. *Am. J. Sci.* 298 (8), 621–672. <https://ajsonline.org/article/60796>.
- Salvador, A., 1994. International stratigraphic guide: a guide to stratigraphic classification, terminology, and procedure. International Union of Geological Sciences and The Geological Society of America, Boulder, Colorado, USA, p. 214.
- Schier, K., Bau, M., Smith, A., Beukes, N.J., Coetzee, L.L., Viehmann, S., 2020. Chemical evolution of seawater in the Transvaal Ocean between 2426 Ma (Ongeluk Large Igneous Province) and 2413 Ma ago (Kalahari Manganese Field). *Gondw. Res.* 88, 373–388. <https://doi.org/10.1016/j.gr.2020.09.001>.
- Senger, M.H., Davies, J., Ovtcharova, M., Beukes, N., Gumsley, A., Gaynor, S.P., Ulianov, A., Ngobeli, R., Schaltegger, U., 2023. Improving the chronostratigraphic framework of the Transvaal supergroup (South Africa) through in-situ and high-precision U–Pb geochronology. *Precamb. Res.* 392, 107070 <https://doi.org/10.1016/j.precamres.2023.107070>.
- Shields, G.A., Strachan, R.A., Porter, S.M., Halverson, G.P., Macdonald, F.A., Plumb, K.A., de Alvarenga, C.J., Banerjee, D.M., Bekker, A., Bleeker, W., Brasier, A., Chakraborty, P.P., Collins, A.S., Condie, K., Das, K., Evans, D.A.D., Ernst, R., Fallick, A.E., Frimmel, H., Fuck, R., Hoffman, P.F., Kamber, B.S., Kuznetsov, A.B., Mitchell, R.N., Poiré, D.G., Poulton, S.W., Riding, R., Sharma, M., Storey, C., Stueeken, E., Tostevin, R., Turner, E., Xiao, S., Zhang, S., Zhou, Y., Zhu, M., 2022. A template for an improved rock-based subdivision of the pre-Cryogenian timescale. *Jgs2020-222 JGS* 179. <https://doi.org/10.1144/jgs2020-222>.
- Shields-Zhou, G.A., Porter, S., Halverson, G.P., 2016. A new rock-based definition for the Cryogenian Period (circa 720–635 Ma). *Episodes* 39, 3–8. <https://doi.org/10.18814/epiiugs/2016/v39i1/89231>.
- Slotznick, S.P., Johnson, J.E., Rasmussen, B., Raub, T.D., Webb, S.M., Zi, J.-W., Kirschvink, J.L., Fischer, W.W., 2022. Reexamination of 2.5-Ga “whiff” of oxygen interglacial points to anoxic ocean before GOE. *Science Advances* 8. doi: 10.1126/sciadv.abj7190.
- Spencer, C.J., Murphy, J.B., Kirkland, C.L., Liu, Y., Mitchell, R.N., 2018. A Paleoproterozoic tectono-magmatic lull as a potential trigger for the supercontinent cycle. *Nat. Geosci.* 11, 97–101. <https://doi.org/10.1038/s41561-017-0051-y>.
- Steadman, J.A., Large, R.R., Blamey, N.J., Mukherjee, I., Corkrey, R., Danyushevsky, L.V., Maslennikov, V., Hollings, P., Garven, G., Brand, U., Lécuyer, C., 2020. Evidence for elevated and variable atmospheric oxygen in the Precambrian. *Precamb. Res.* 343, 105722 <https://doi.org/10.1016/j.precamres.2020.105722>.
- Strand, K., 2012. Global and continental-scale glaciations on the Precambrian earth. *Mar. Pet. Geol.* 33, 69–79. <https://doi.org/10.1016/j.marpetgeo.2012.01.011>.
- Strand, K.O., Laajoki, K., 1993. Paleoproterozoic glaciomarine sedimentation in an extensional tectonic setting: the Honkala Formation, Finland. *Precamb. Res.* 64, 253–271. [https://doi.org/10.1016/0301-9268\(93\)90080-L](https://doi.org/10.1016/0301-9268(93)90080-L).
- Stüeken, E.E., Buick, R., Anbar, A.D., 2015. Selenium isotopes support free O₂ in the latest Archean. *Geology* 43, 259–262. <https://doi.org/10.1130/G36218.1>.
- Takehara, M., Komure, M., Kiyokawa, S., Horie, K., Yokohama, K., 2010. Detrital zircon SHRIMP U–Pb age of the 2.3 Ga diamictites of the Meteorite Bore Member in the South Pilbara, Western Australia, in: Fifth International Archean Symposium Abstracts. Fifth International Archean Symposium, Perth, Western Australia. 5–9 September 2010. Geological Survey of Western Australia, pp. 223–224.
- Thibon, F., Blichert-Toft, J., Albarede, F., Foden, J., Tsikos, H., 2019. A critical evaluation of copper isotopes in Precambrian Iron Formations as a paleoceanographic proxy. *Geochim. Cosmochim. Acta* 264, 130–140. <https://doi.org/10.1016/j.gca.2019.08.020>.
- Thorne, A.M., Trendall, A.F., 2001. Geology of the Fortescue Group, Pilbara Craton, Western Australia. Geological Survey of Western Australia, p. 249.
- Thorne, A.M., Tyler, I.M., 1996. Geology of the Rocklea 1:100 000 sheet. Geological Survey of Western Australia 15, pp.
- Trendall, A.F., 1984. The Archean/Proterozoic transition as a geological event — a view from Australian evidence. In: Holland, H.D., Trendall, A.F. (Eds.), *Patterns of Change in Earth Evolution: Report of the Dahlem Workshop on Patterns of Change in Earth Evolution*, Berlin 1983, May 1–6. Springer-Verlag, Berlin Heidelberg New York Tokyo, pp. 243–259.
- Trendall, A.F., 1995. The Woongarra Rhyolite - a giant lavalike felsic sheet in the Hamersley Basin of Western Australia. Geological Survey of Western Australia 70, pp.
- Trendall, A.F., Blockley, J.G., 1970. The iron formations of the Precambrian Hamersley Group, Western Australia, with special reference to the associated crocidolite. Geological Survey of Western Australia 366 pp.
- Trendall, A.F., Compston, W., Nelson, D.R., de Laeter, J.R., Bennett, V.C., 2004. SHRIMP zircon ages constraining the depositional chronology of the Hamersley Group, Western Australia. *Aust. J. Earth Sci.* 51, 621–644.
- Trendall, A.F., 1979. A revision of the Mount Bruce Supergroup, in: Annual report for the year 1978. Geological Survey of Western Australia, pp. 63–71.
- Uveges, B.T., Izon, G., Ono, S., Beukes, N.J., Summons, R.E., 2023. Reconciling discrepant minor sulfur isotope records of the Great Oxidation Event. *Nat Commun* 14, 279. <https://doi.org/10.1038/s41467-023-35820-w>.
- Van Kranendonk, M.J., Altermann, W., Beard, B.L., Hoffman, P.F., Johnson, C.M., Kasting, J.F., Melezhik, V.A., Nutman, A.P., Papineau, D., Pirajno, F., 2012. Chapter 16 – A chronostratigraphic division of the Precambrian: possibilities and challenges. In: Gradstein, F.M., Ogg, J.G., Schmitz, M., Ogg, G.M. (Eds.), *The Geologic Time Scale*. Elsevier B.V., Amsterdam, The Netherlands, pp. 299–392.
- Van Kranendonk, M.J., Altermann, W., Mazumder, R., 2015a. A squall by the seashore ca 2.3 billion years ago: raindrop imprints in a Paleoproterozoic tidal flat deposit, Kungarra Formation, Western Australia. *Aust. J. Earth Sci.* 62, 265–274. <https://doi.org/10.1080/08120099.2015.1016105>.

- Van Kranendonk, M.J., Mazumder, R., 2015. Two Paleoproterozoic glacio-eustatic cycles in the Turee Creek Group, Western Australia. *Geol. Soc. Am. Bull.* 127, 596–607.
- Van Kranendonk, M.J., Smithies, R.H., Hickman, A.H., Champion, D.C., 2007. Review: Secular tectonic evolution of Archean continental crust: interplay between horizontal and vertical processes in the formation of the Pilbara Craton, Australia. *Terra Nova* 19, 1–38.
- Van Kranendonk, M.J., Mazumder, R., Yamaguchi, K.E., Yamada, K., Ikehara, M., 2015b. Sedimentology of the Paleoproterozoic Kungarra Formation, Turee Creek Group, Western Australia: a conformable record of the transition from early to modern Earth. *Precamb. Res.* 256, 314–343.
- Van Kranendonk, M.J., 2003. Stratigraphic and tectonic significance of eight local unconformities in the Fortescue Group, Pear Creek Centrocline, Pilbara Craton, Western Australia, in: Geological Survey of Western Australia Annual Review 2001–02. Geological Survey of Western Australia, pp. 70–79.
- Warke, M.R., Schröder, S., Strauss, H., 2018. Testing models of pre-GOE environmental oxidation: a Paleoproterozoic marine signal in platform dolomites of the Tongwane Formation (South Africa). *Precamb. Res.* 313, 205–220. <https://doi.org/10.1016/j.precamres.2018.04.015>.
- Warke, M.R., Schröder, S., 2018. Synsedimentary fault control on the deposition of the Deutschland Formation (South Africa): Implications for depositional settings, Paleoproterozoic stratigraphic correlations, and the GOE. *Precamb. Res.* 310, 348–364. <https://doi.org/10.1016/j.precamres.2018.03.001>.
- Warke, M.R., Di Rocco, T., Zerkle, A.L., Lepland, A., Prave, A.R., Martin, A.P., Ueno, Y., Condon, D.J., Claire, M.W., 2020. The Great Oxidation Event preceded a Paleoproterozoic “snowball Earth”. *PNAS* 117, 13314–13320. <https://doi.org/10.1073/pnas.2003090117>.
- Wille, M., Kramers, J.D., Nägler, T.F., Beukes, N.J., Schröder, S., Meisel, T., Lacassie, J.P., Voegelin, A.R., 2007. Evidence for a gradual rise of oxygen between 2.6 and 2.5 Ga from Mo isotopes and Re-PGE signatures in shales. *Geochim. Cosmochim. Acta* 71, 2417–2435.
- Williford, K.H., Ushikubo, T., Lepot, K., Kitajima, K., Hallmann, C., Spicuzza, M.J., Kozdon, R., Eigenbrode, J.L., Summons, R.E., Valley, J.W., 2016. Carbon and sulfur isotopic signatures of ancient life and environment at the microbial scale: Neoproterozoic shales and carbonates. *Geobiology* 14, 105–128. <https://doi.org/10.1111/gbi.12163>.
- Windley, B.F., 1984. *The Evolving Continents*, 2nd ed. John Wiley and Sons Ltd, U.K., p. 399.
- Wingate, M.T.D., 1998. A palaeomagnetic test of the Kaapvaal – Pilbara (Vaalbara) hypothesis at 2.78 Ga. *S. Afr. J. Geol.* 101, 257–274.
- Wingate, M.T.D., Lu, Y., Kirkland, C.L., Johnson, S.P., 2018a. 195892: rhyodacite, Woongarra Pool. *Geochronology Record* 1453, 4 pp. www.dmirs.wa.gov.au/geochron.
- Wingate, M.T.D., Lu, Y., Martin, D.McB., 2018b. 156347: sandstone, Mount Wall. *Geochronology Record* 1481, 6 pp. www.dmirs.wa.gov.au/geochron.
- Wingate, M.T.D., Lu, Y., Martin, D.McB., 2020. 225701: volcaniclastic siltstone, Fish Pool. *Geochronology Record* 1681, 4 pp. www.dmirs.wa.gov.au/geochron.
- Wingate, M.T.D., Fielding, I.O.H., Lu, Y., Martin, D.McB., 2021a. 225758: tuffaceous volcanic rock, Wittenoorn Gorge. *Geochronology Record* 1812, 4 pp. www.dmirs.wa.gov.au/geochron.
- Wingate, M.T.D., Fielding, I.O.H., Lu, Y., Martin, D.McB., 2021b. 225760: tuffaceous volcanic rock, Wittenoorn Gorge. *Geochronology Record* 1813, 4 pp. www.dmirs.wa.gov.au/geochron.
- Young, G.M., 1978. Some aspects of the evolution of the Archean crust. *Geosci. Can.* 5, 140–149.
- Young, G.M., 2019. Aspects of the Archean-Proterozoic transition: how the great Huronian Glacial Event was initiated by rift-related uplift and terminated at the rift-drift transition during break-up of Lauroscandia. *Earth Sci. Rev.* 190, 171–189. <https://doi.org/10.1016/j.earscirev.2018.12.013>.